1-1-1968

Optimizing activity separation in fission product decay chains

Jay Harold Norman
Iowa State University

OPTIMIZING ACTIVITY SEPARATION IN FISSION PRODUCT DECAY CHAINS

by

Jay Harold Norman

A Thesis Submitted to the
Graduate Faculty in Partial Fulfillment of
The Requirements for the Degree of
MASTER OF SCIENCE

Major Subject: Nuclear Engineering

Iowa State University
Of Science and Technology
Ames, Iowa

1968

TABLE OF CONTENTS

INTRODUCTION

An isotope separator system called "TRISTAN" (5, 9) has been developed to study short-lived activities produced at the Ames Laboratory Research Reactor. As shown in Figure 1, TRISTAN currently consists of a fissionable source located in a reactor beam tube, a transport line to the ion source, the isotope separator, a collector box where the mass desired is selected, and a switching magnet which directs the ion beam to one of five detection stations where the ions are deposited. The radioactive ions are then studied by suitable detectors. The types of studies that can be made with the system include half life determination, measurement of beta and gamma-ray spectra, and measurement of delayed neutron emission from fission product precursors. The system operates on-line with the reactor and can provide a continuous supply of single mass radioactive ions at the desired detector station.

Since the radioactive nuclides produced are primary fission products they are relatively far from the stability line and can give rise to long decay chains. Thus, even though the isotope separator can continue to supply radioactive ions to the detector station to compensate for decay, the buildup of the daughter product activities soon creates an intolerable background from an analysis standpoint. Thus a device is required at the detection point that will provide a method of separating the activities of the individual isobars of a particular decay chain.

One method for accomplishing an isobaric separation is to place a movable tape at the detector station and allow the isotope separator beam to be deposited on the tape. A device called a moving tape collector has

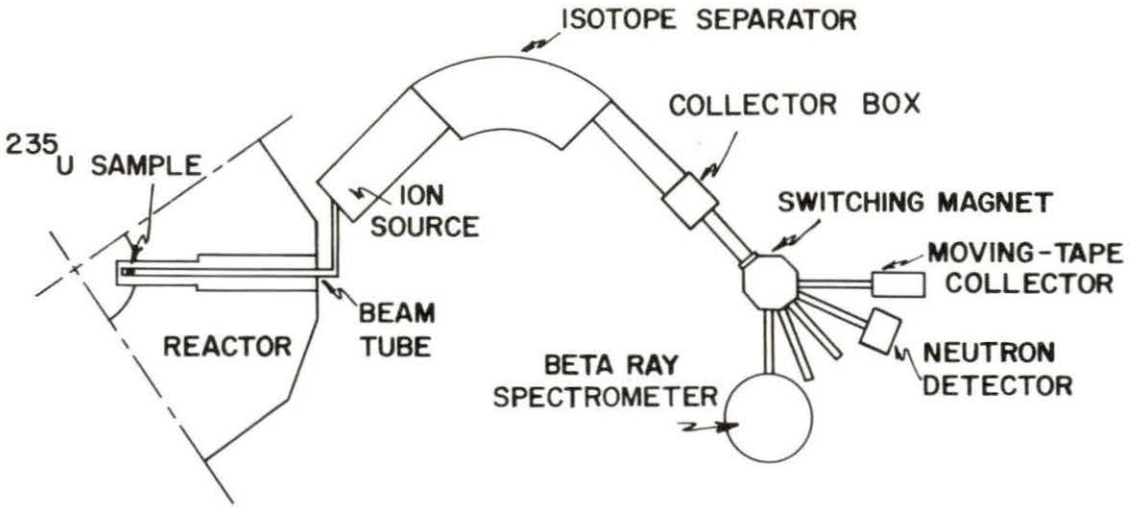

Figure 1. Layout of TRISTAN on-line isotope separator system

been designed and built for this purpose by the Mechanical Engineering Section of the Ames Laboratory Reactor Division.

In the work which follows, the general problem of determining the method of operation of such a device for obtaining optimum activity separation of each member of a decay chain is investigated. The characteristics peculiar to the moving tape collector installed in the TRISTAN system are presented. Tables are given which show the maximum activity separation corresponding to the optimum method of operation of the moving tape collector for all fission product decay chains capable of being produced by the source.

REVIEW OF LITERATURE

The problem of continuously separating the activities of isobars in long decay chains was first encountered in the application of isotope separators to the study of fission product activities. Prior to that development it was not possible to produce such activities. Since the application of on-line isotope separation techniques to the study of short-lived activities is a relatively recent development, very little has been published concerning the problem of isobaric activity separation at the detector station.

Borg et al. (3), in reporting on experiences with a similar isotope separator system, describe a moving tape collector which uses a closed loop of tape driven at a constant speed. The device was successful in separating the activities of two-member decay chains.

A group at Princeton University, Sidenius et al. (8), has designed a moving tape collector of open loop design to separate the activities of short-lived products from Cf^{252} spontaneous fission. The device has been applied to the Xe^{140} and Xe^{142} decay chains (1).

Finally, Crancon and Moussa (4), working with a reactor on-line isotope separator at the Commissariat a l'Energie Atomique in France, have reported on a time sequencing technique for accomplishing activity separation of the Kr^{94} decay chain but do not report any results from the use of moving tape collector separation techniques.

DESCRIPTION OF THE MOVING TAPE COLLECTOR

Introduction

The moving tape collector is a high vacuum box that contains a tape transport system, penetrations for the ion beam input and vacuum pump connection, mounts for detector placement, and shielding material. Figure 2 is a photograph of the tape collector with a side panel, some of the internal shielding, and the tape reel cover removed. Note that the tape supply and take-up reels are the standard 7 inch diameter size.

Figure 3 shows vertical and horizontal cross section detail drawings of the tape collector. Aluminum construction is used throughout unless otherwise noted. The main body of the device is a hollow box 15.75 inches by 14 inches by 6 inches. Four detector mounts, a beam input tube, a vacuum connection, a tape reel support, a tape reel cover, and the tape drive motor are attached to the outside of the box. The tape transport mechanism, lead shielding, and detector collimators are mounted inside the box.

The Tape Transport System

The tape transport system consists of a drive motor, the internal tape transport mechanism including the supply and take-up reels, and the tape itself. The drive motor used is a Slo-Syn, model SS50-1009, stepping motor. The motor is operated by a drive unit that supplies appropriate voltage pulses to the motor such that 200 pulses (or steps) are required to rotate the motor shaft through one revolution. By counting the total number of input voltage steps to the motor the total angle of rotation of the shaft can be calculated. Likewise, the input step rate determines the

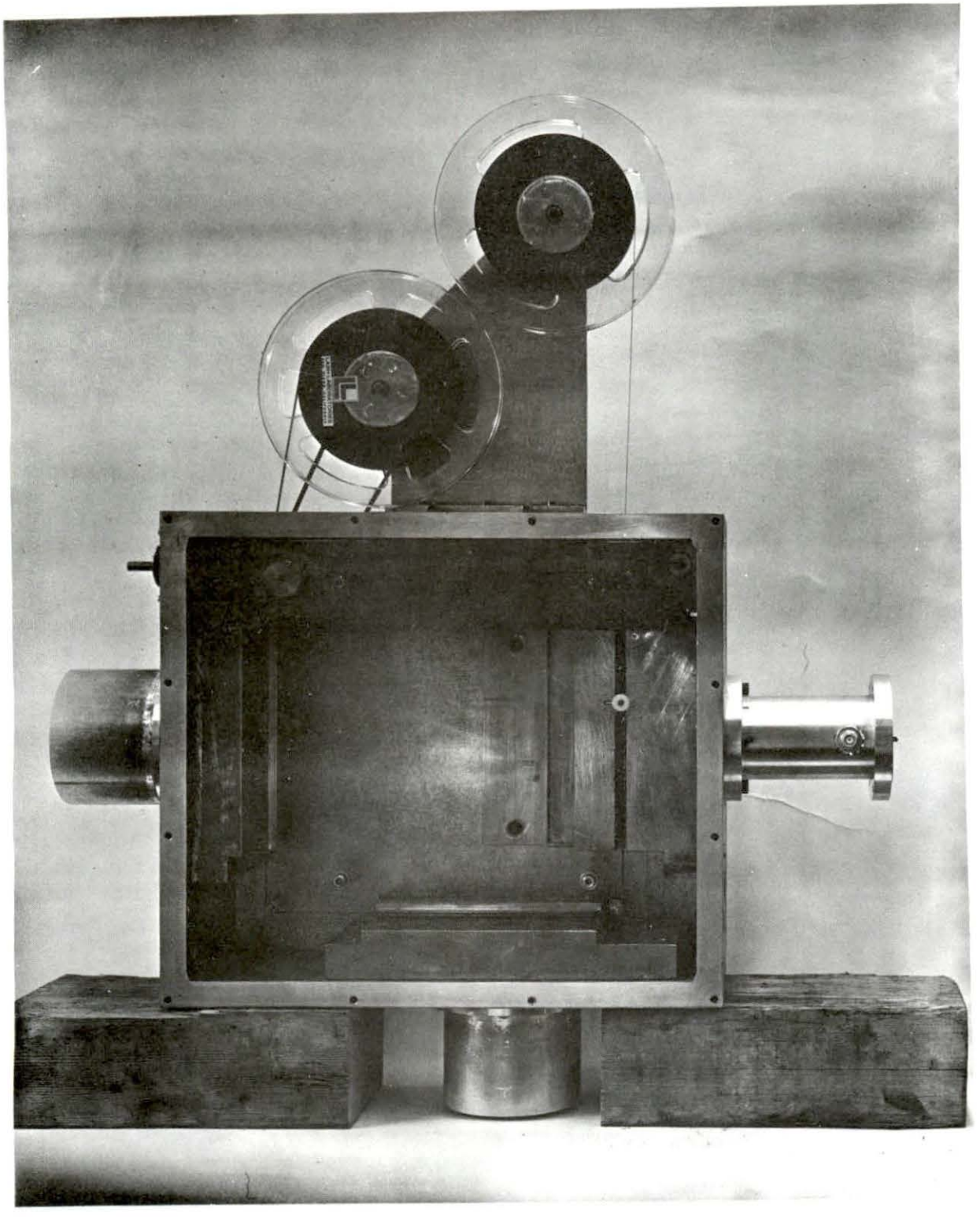

Figure 2. View of moving tape collector

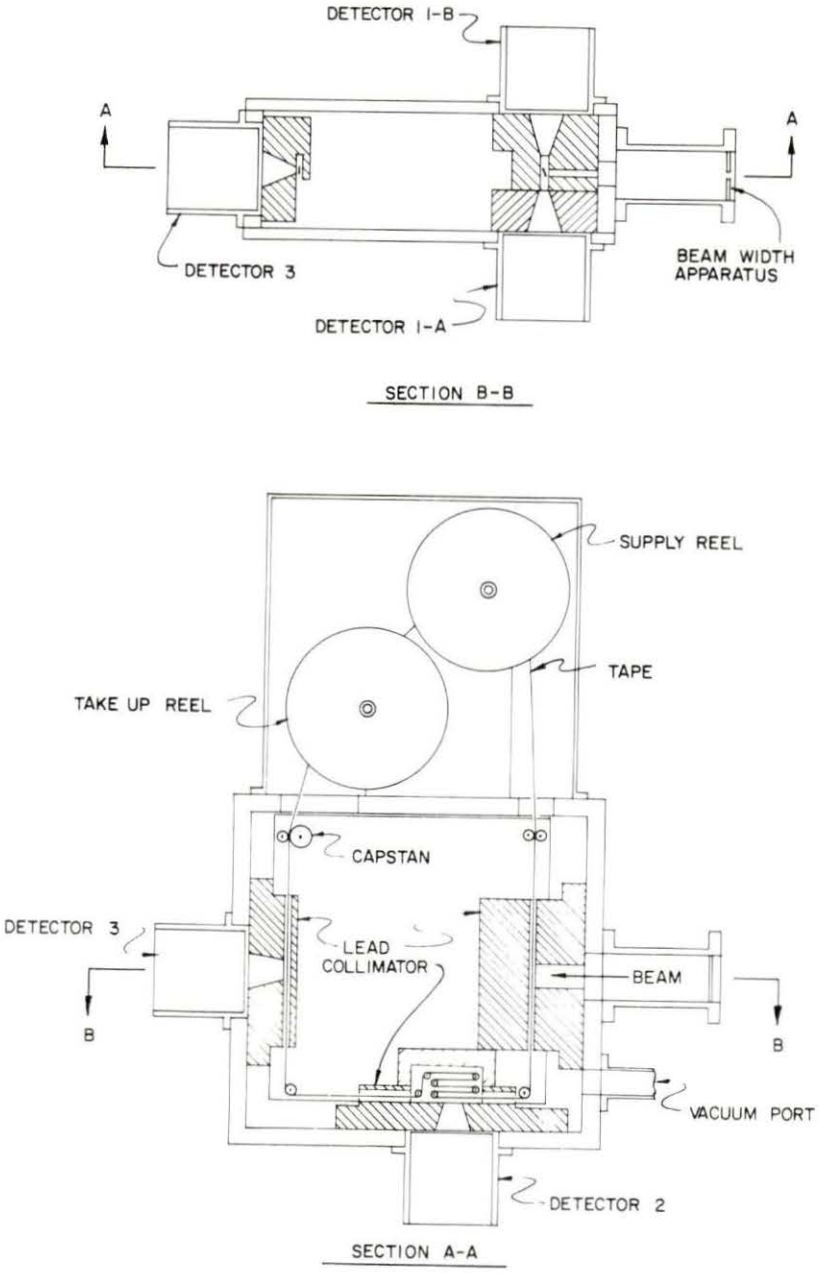

Figure 3. Vertical and horizontal cross sections through the moving tape collector

angular velocity of the motor shaft. A stepping motor provides a precise method of shaft positioning and shaft speed adjustments so long as the torque load to the shaft remains within the motor torque limitations.

The internal tape transport mechanism is supported by a Lexan plastic mounting plate (for the purpose of electrical isolation to enable ion beam current measurement) and consists of a nominal one-inch diameter capstan, a spring loaded backing roller, and several additional guide rollers located around the tape track to insure proper tape position and alignment. The stepping motor drives the capstan via a vacuum rotary-motion feedthrough. The capstan surface is coated with a rubber base compound to reduce slippage and the spring loaded backing roller helps to insure good contact between the tape and the capstan. The tape supply and take-up reels are provided with mechanical slip clutches that are adjusted to maintain proper tape tension. The take-up reel drive is provided by an O-ring belt connected to the capstan shaft. Thus, during operation the tape moves from the supply reel, past the beam deposit point, around the periphery of the box, over the capstan, and onto the take-up reel.

The tape used in the moving tape collector is a 0.25 inch, Kapton-base tape with a metalized coating consisting of a cobalt and nickel alloy. The tape (Pyrotrack, manufactured by Lash Laboratories, San Diego, California) is designed for high temperature applications and it was selected because the metalized conducting coating is useful for measuring the ion current when the beam is being deposited on the tape. Also, the high temperature properties reduce the possibility of the tape being distorted from local heating by the ion beam at the point of deposit.

Detector Arrangement

The moving tape collector provides four detector positions. Each detector position includes an external detector mounting port, an internal lead collimator that provides a view of a small portion of the tape, and additional internal shielding to minimize the detection of activity from other portions of the tape. As shown in the upper half of Figure 3, there are two detector positions located at the centerline of the beam deposit point; they are designated 1-A and 1-B. The lower half of Figure 3 shows the locations of detectors 2 and 3, which can be used for simultaneous analysis of long-lived activities.

At each detector location a 3 inch diameter hole is provided in the tape collector box wall and the detector mounting port is attached with a vacuum seal. The detector mount is a 3.5 inch inside diameter by 3 inch deep receptacle with a 0.0625 inch thick end plate facing the lead collimator. The distance from the detector mount end plate to the center line of the tape is 3 inches at positions 1-A and 1-B and 2.25 inches at positions 2 and 3. Each detector mount can accomodate both NaI(Tl) and Ge(Li) gamma-ray detectors. Position 1-B can be made to accommodate a beta-ray detector (plastic scintillator or Si(Li) detector).

The collimators at position 1-A and 1-B consist of a machined, tapered hole through the 1.75 inch thick lead shield placed between the detector mount end plate and the tape. The collimator holes have the approximate dimensions of 0.25 inches by 0.75 inches on the side facing the tape which expands to a circle of one inch diameter on the side facing the detector. The collimator holes at positions 2 and 3 have approximately the same dimensions except that the lead shields are 1.375 inches thick.

At the point of beam deposit (i.e., at the center line of detector positions 1-A and 1-B) the tape is rotated 30^{o} out of its plane of travel to increase the source area presented to the detectors. An equivalent tape width of 0.125 inches (as viewed by the detectors) is produced and the direction of rotation is such that the activity observed at position 1-A must pass through the tape while the detector at 1-B views the deposit point directly. The centerlines of detectors 2 and 3 are perpendicular to the plane of the tape.

Types of Operation

The moving tape collector can be operated either continuously or discontinuously. Continuous operation is used when it is desired to move the tape at some required velocity and discontinuous operation is used when it is desired to move the tape some required total distance.

Continuous operation is accomplished by supplying a constant pulse rate to the motor drive unit causing the tape to move at a constant number of steps per unit time. In the discontinuous mode the tape can be moved a desired distance from some initial position by supplying a known total number of pulses to the motor drive unit.

THEORETICAL DEVELOPMENT

The buildup and decay of the activity deposited on the tape of a moving tape collector is exactly analogous to the continuous buildup and decay of activity in fission product decay chains.

An example is the following simple decay chain in which the production term is limited to the first member.

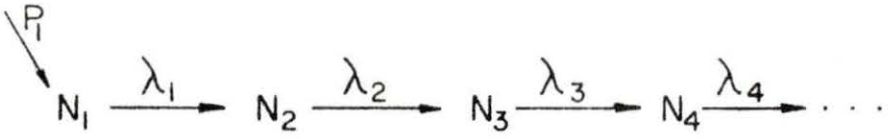

(1)

The total amount of any chain member at any time is given by the familiar Bateman (2) equation which can be written in the following contemporary form

$$N_i(T,\tau_d) = \lambda_1 \lambda_2 \cdots \lambda_{i-1} P_1 \sum_{j=1}^{i} \frac{(1-e^{-\lambda_j T}) e^{-\lambda_j \tau_d}}{\lambda_j \prod_{k \neq j} (\lambda_k - \lambda_j)} \tag{2}$$

where

T = buildup time

τ_d = decay time

λ_i = decay constant for the i-th member of the chain

P_1 = production rate of the first member of the chain

A more useful form of Equation 2 gives the activity of any chain member at any time as

$$A_i(T,\tau_d) = \lambda_i N_i(T,\tau_d) = \lambda_1 \lambda_2 \cdots \lambda_i P_1 \sum_{j=1}^{i} \frac{(1-e^{-\lambda_j T}) e^{-\lambda_j \tau_d}}{\lambda_j \prod_{k \neq j} (\lambda_k - \lambda_j)} \tag{3}$$

In general, the buildup and decay of fission products in a fissionable source is complicated by the addition of production terms all along the decay chain. Wahl et al. (10) show that the nuclear charge distribution for any mass number, A, is approximately Gaussian about the most probable charge, Z_p. Thus the actual decay chain can be shown schematically as

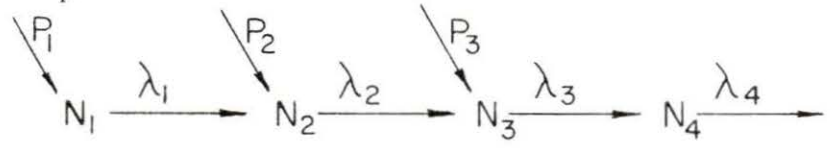

(4)

The above decay scheme can be represented as the sum of the three partial decay schemes shown below

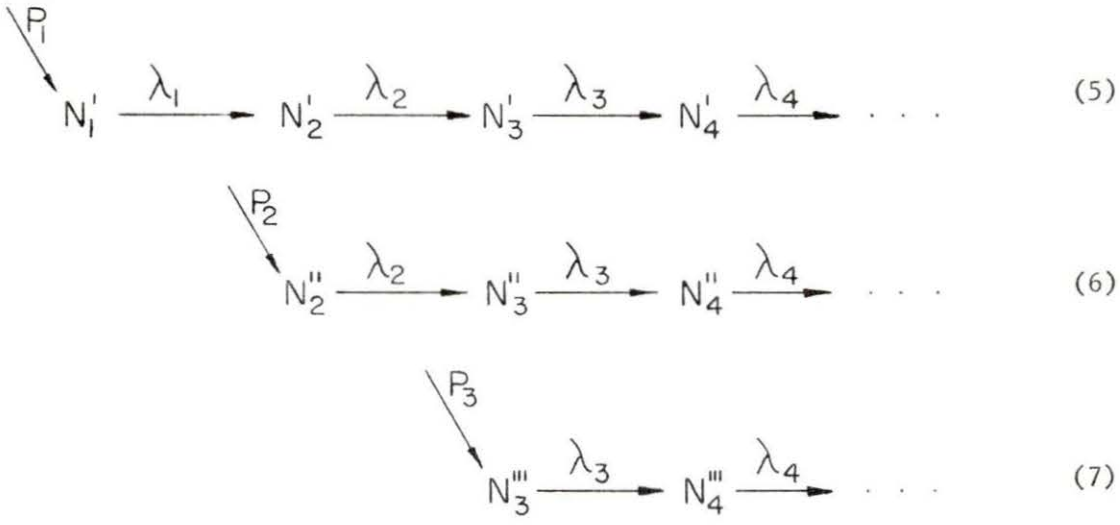

(5)

(6)

(7)

The solution for the total activity of any member of the general scheme 4, is just the sum of that activity in each of the partial schemes, 5, 6, and 7. The solutions for the partial decay schemes are given by Equation 3 above. The solution for scheme 5 is

$$A_i^{(1)}(T,\tau_d) = \lambda_1 \lambda_2 \cdots \lambda_i P_1 \sum_{j=1}^{i} \frac{(1-e^{-\lambda_j T})e^{-\lambda_j \tau_d}}{\lambda_j \prod_{k \neq j} (\lambda_k - \lambda_j)} \tag{8}$$

where the superscript indicates the activity due to the production term P_1.

For scheme 6 the solution is

$$A_i^{(2)}(T,\tau_d) = \lambda_2\lambda_3\cdots\lambda_i P_2 \sum_{j=2}^{i} \frac{(1-e^{-\lambda_j T})e^{-\lambda_j \tau_d}}{\lambda_j \prod_{k\neq j}(\lambda_k-\lambda_j)} \tag{9}$$

Similarly for scheme 7

$$A_i^{(3)}(T,\tau_d) = \lambda_3\lambda_4\cdots\lambda_i P_3 \sum_{j=3}^{i} \frac{(1-e^{-\lambda_j T})e^{-\lambda_j \tau_d}}{\lambda_j \prod_{k\neq j}(\lambda_k-\lambda_j)} \tag{10}$$

The total activity for any member of scheme 4 is then

$$A_i(T,\tau_d) = A_i^{(1)}(T,\tau_d) + A_i^{(2)}(T,\tau_d) + A_i^{(3)}(T,\tau_d) + \cdots = \sum_{m=1}^{L} A_i^{(m)}(T,\tau_d) \tag{11}$$

where L = number of production terms.

Substituting Equations 8, 9, and 10 into Equation 11 yields

$$A_i(T,\tau_d) = \sum_{m=1}^{L} \left\{ \lambda_m\lambda_{m+1}\cdots\lambda_i P_m \sum_{j=m}^{i} \frac{(1-e^{-\lambda_j T})e^{-\lambda_j \tau_d}}{\lambda_j \prod_{k\neq j}(\lambda_k-\lambda_j)} \right\} \tag{12}$$

where

i = ith member of the decay chain

m = mth production term

L = number of production terms

$i \geq m$

Since the separation of activities is determined by the ratio of the activity of the member of interest to the total activity present, the expression desired is

$$R_i(T,\tau_d) = A_i(T,\tau_d) \Big/ \sum_{i=1}^{N} A_i(T,\tau_d) \tag{13}$$

where N is the total number of members in the decay chain and $A_i(T,\tau_d)$ is defined by Equation 12.

When a detector is used to observe the activity of a decay chain member the measurement requires a finite period of time called the count time, τ_c. Let $D_i(T,\tau_d,\tau_c)$ be the integrated activity over the count time, thus

$$D_i(T,\tau_d,\tau_c) = \int_{\tau_d}^{\tau_d+\tau_c} A_i(T,\tau)\,d\tau \tag{14}$$

Now substituting for $A_i(T,\tau_d)$ from Equation 12 and performing the indicated operation yields

$$D_i(T,\tau_d,\tau_c) = \sum_{m=1}^{L} \left\{ \lambda_m \lambda_{m+1} \cdots \lambda_i P_m \sum_{j=m}^{i} \frac{(1-e^{-\lambda_j T})(1-e^{-\lambda_j \tau_c})e^{-\lambda_j \tau_d}}{\lambda_j^2 \prod_{k\neq j}(\lambda_k - \lambda_j)} \right\} \tag{15}$$

The ratio of the individual integrated activity to the total integrated activity is a measure of the separation obtained during the measurement period. Let $S_i(T,\tau_d,\tau_c)$ be the ratio defined by

$$S_i(T,\tau_d,\tau_c) = D_i(T,\tau_d,\tau_c) \Big/ \sum_{i=1}^{N} D_i(T,\tau_d,\tau_c) \tag{16}$$

Equations 12, 13, 15, and 16 describe the buildup, decay, and total observable disintegrations on a moving tape subject to activity deposition by a beam from a mass separator where T is taken to be the beam deposition time, τ_d the subsequent delay time, and τ_c the total count time.

ANALYTICAL SOLUTION AND OPTIMIZATION SCHEME

In this section the methods of solution of Equations 12, 13, 15, and 16 are presented. The optimization scheme is then outlined.

Method of Analytical Solution

A computer program called ISOBAR was written for the IBM-360-65 computer. It calculates the value of $A_i(T,\mathcal{T}_d)$, $R_i(T,\mathcal{T}_d)$, $D_i(T,\mathcal{T}_d,\mathcal{T}_c)$, and $S_i(T,\mathcal{T}_d,\mathcal{T}_c)$ (as given by Equations 12, 13, 15, and 16 respectively) for any selected value of T, $\mathcal{T}_d$, or $\mathcal{T}_c$ and for all i such that $1 \leq i \leq N$. The program listing and flow chart for ISOBAR are given in Appendix A.

The buildup and decay scheme shown in Equation 4 is a schematic representation of the following coupled differential equations.

$$\begin{aligned} \dot{N}_1 &= P_1 - \lambda_1 N_1 \\ \dot{N}_2 &= P_2 + \lambda_1 N_1 - \lambda_2 N_2 \\ \dot{N}_3 &= P_3 + \lambda_2 N_2 - \lambda_3 N_3 \\ &\vdots \qquad\qquad \vdots \end{aligned} \tag{17}$$

The Equations 17 can be rewritten as activity equations to yield

$$\begin{aligned} \dot{A}_1 &= \lambda_1 P_1 - \lambda_1 A_1 \\ \dot{A}_2 &= \lambda_2 P_2 + \lambda_2 A_1 - \lambda_2 A_2 \\ \dot{A}_3 &= \lambda_3 P_3 + \lambda_3 A_2 - \lambda_3 A_3 \\ &\vdots \qquad\qquad \vdots \end{aligned} \tag{18}$$

Since the Equations 18 are well suited to analog computer solution, an analog technique was used to check the operation of the ISOBAR program. Appendix B shows the analog wiring diagram, magnitude scaled equations,

and the agreement obtained for a fictitious test decay chain. The analog solutions shown in Appendix B verified the operation of the ISOBAR program for total activity calculations.

The ISOBAR program is written in double precision and provides a rapid and accurate calculation of the activity separation and integrated activity ratio of all members of a given decay chain when provided with the magnitudes of the production terms, the decay chain member half-lives, and the values of T, τ_d, and τ_c.

Included in the ISOBAR program is a subroutine called CALTAB. The subroutine calculates and prints out a table of values of $R_i(T,\tau_d)$ and the fractional saturated activity of $A_i(T,\tau_d)$ for $(t_{\frac{1}{2}})_i/10 \leq \tau_d \leq 10(t_{\frac{1}{2}})_i$ and $(t_{\frac{1}{2}})_i/1000 \leq T \leq 10(t_{\frac{1}{2}})_i$ where $(t_{\frac{1}{2}})_i$ is the halflife in seconds of the i-th member of the decay chain. The table provides a rapid visual method of determining the approximate region where the maximum value of $R_i(T,\tau_d)$ occurs.

Optimization Scheme

As noted above, if the count time is disregarded the optimum activity separation for any member of a given decay chain is obtained when $R_i(T,\tau_d)$ of Equation 13 is a maximum. The function $R_i(T,\tau_d)$ is a surface above the T-τ_d plane. The optimization scheme defines a procedure for finding the T and τ_d that yields the highest point on the surface.

An iterative technique using a steepest ascent method was indicated and the formulation by McElhone (7) was employed. Using an initial estimate for T and τ_d obtained from the ISOBAR program, a point on the surface is calculated. From that point a unit vector is generated that points in the direction of steepest ascent along the surface. An arbitrarily

specified step size is then impressed on the unit vector and new values of T and τ_d obtained. A new $R_i(T,\tau_d)$ is calculated and compared to the previous value. If the new ratio is greater the values of T and τ_d are stored and a new unit vector is calculated. If the new ratio is smaller then the step size is decreased and other trial values of T and τ_d are calculated. The process continues until no further improvement in $R_i(T,\tau_d)$ is obtained. Then the maximum value of $R_i(T,\tau_d)$ and the corresponding values of T and τ_d are printed out and the procedure is repeated for the next member of the decay chain. Examination of the output of CALTAB indicates the existance of only a single maximum.

A program called ISOMAX was written for the IBM-360-65 that performs the optimization iterative procedure. The program listing for ISOMAX is given in Appendix C.

DISCUSSION OF EXPERIMENTAL RESULTS

Introduction

When the moving tape collector is operated in the continuous mode the optimization times T and τ_d calculated by ISOMAX and the counting times τ_c can be related to the tape collector operational parameters by appropriate equations. The results of the measured tape collector parameters and the equations relating them to the optimization times are presented in this section.

When the tape collector is operated in the discontinuous mode the primary concern is that the tape is transported over the required distance without slippage or missed steps. Appropriate measurements were made to verify the positioning accuracy of the device.

The maximum attainable activity separation at each detector station is also determined by the internal shielding arrangement. Cross detection is defined as the detection of tape activity when the active portion of the tape is located at some position other than in front of the lead collimator aperture of the detector in use. The cross detection properties are a direct measure of the internal shielding effectiveness.

The results of the measurements of the mechanical properties and performance and the cross detection characteristics of the moving tape collector are presented in this section.

Moving Tape Collector Parameters

Definition of parameters

If the tape collector parameters are defined as follows:

D = Capstan diameter (inches)

C = Motor constant (200 steps/revolution)

K = Proportionality constant (steps/inch)

h = Ion beam height (inches)

D_2 = Distance from centerline of detector 1 to 2 (inches)

D_3 = Distance from centerline of detector 1 to 3 (inches)

a_1 = Lead collimator aperture at detector 1 (inches)

a_2 = Lead collimator aperture at detector 2 (inches)

a_3 = Lead collimator aperture at detector 3 (inches)

$(a_i)_{eff}$ = Effective lead collimator aperture at detector i (inches)

and the variables of interest are defined by

F = Motor drive input pulse rate (steps/second)

V = Tape speed (inches/second)

T = Collection time at beam deposit point

$(\tau_d)_1$ = Delay during counting period at detector 1

$(\tau_d)_i$ = Delay time from end of beam deposit to start of detection period (seconds); i = 2, 3

$(\tau_c)_i$ = Counting time at detector (seconds); i = 1, 2, 3

Then the following relationships hold

$$V = \frac{F \pi D}{C} \tag{19}$$

$$T = \frac{h}{V} \tag{20}$$

$$(\tau_d)_1 = \frac{a_1 - h}{2V} \tag{21}$$

$$(\tau_d)_i = \frac{D_i - 1/2(h + a_i)}{V} \quad ; \quad i = 2,3 \tag{22}$$

$$(\tau_c)_i = \frac{(a_i)_{eff}}{V} \quad ; \quad i = 1,2,3 \tag{23}$$

Aperture control device

Figure 4 shows an enlarged view of the tape path in the vicinity of detector position 2. The device shown provides a method of increasing the effective aperture of the lead collimator at detector 2 by doubling the tape back a maximum of four times requiring the deposited activity on the tape to make a total of five passes past the collimator. The aperture control device can also be threaded for three passes or a single pass past the collimator opening. Thus, the effective aperture is defined as

$$(a_2)_{eff} = C_k a_2 \quad ; \quad k = 1,3,5 \tag{24}$$

where the k subscript indicates the number of passes. Note that $C_1 = 1$ and the value of $(a_2)_{eff}$ for k = 3 and 5 are given in the next section. Since no provision for aperture control is provided at detectors 1 and 3, $(a_1)_{eff} = a_1$ and $(a_3)_{eff} = a_3$.

Measurements and results

Figure 5 shows the experimental arrangement used to measure the tape collector constants. The signal to the motor drive unit (Slo-Syn Translator) was fed from a square wave oscillator through a relay. The relay was controlled by the timer-scaler unit such that when the timer was in operation the relay closed. The signal from the oscillator was simultaneously fed to the scaler portion of the timer-scaler unit which recorded the total number of pulses sent to the motor drive unit. The control for the motor, timer, and scaler was provided by the timer.

The tape was marked and aligned at some initial position; for example, with the mark at the centerline of detector position 1. The tape was then

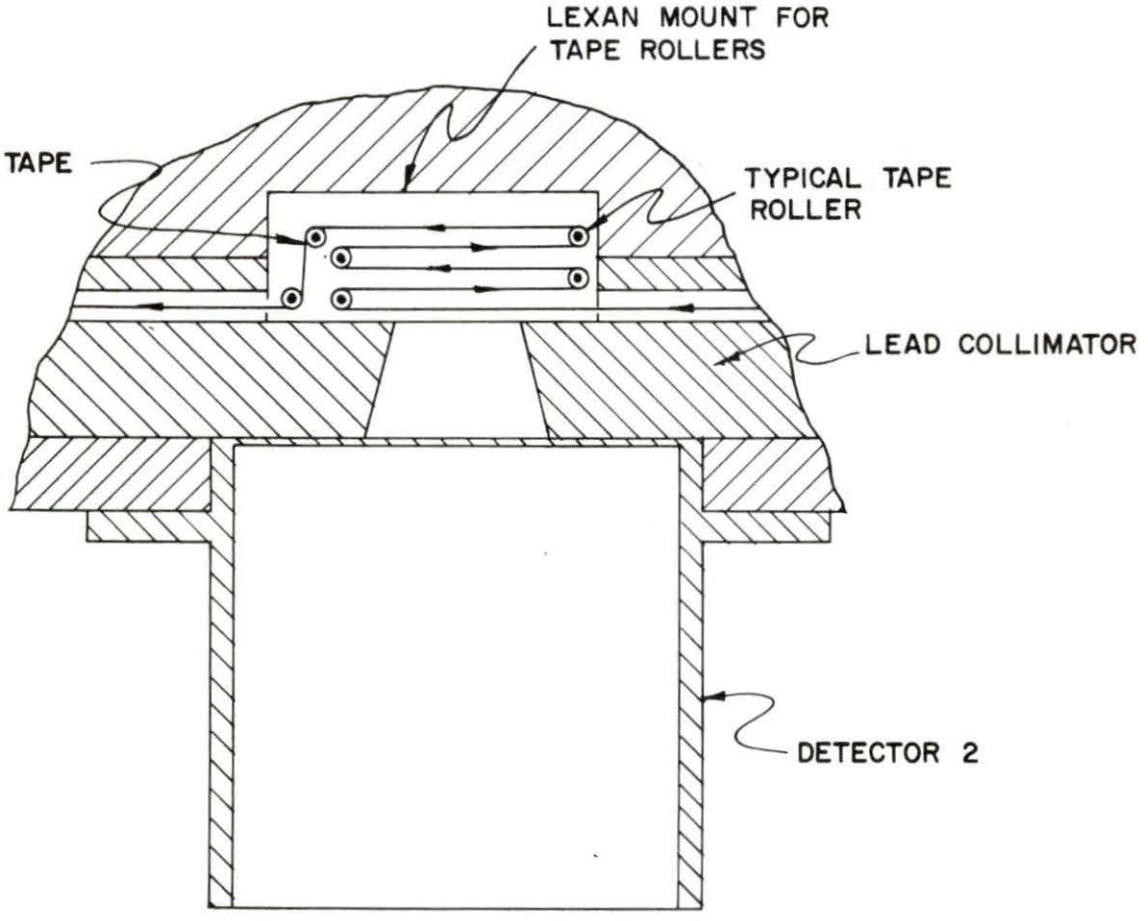

Figure 4. Aperture control device at detector 2

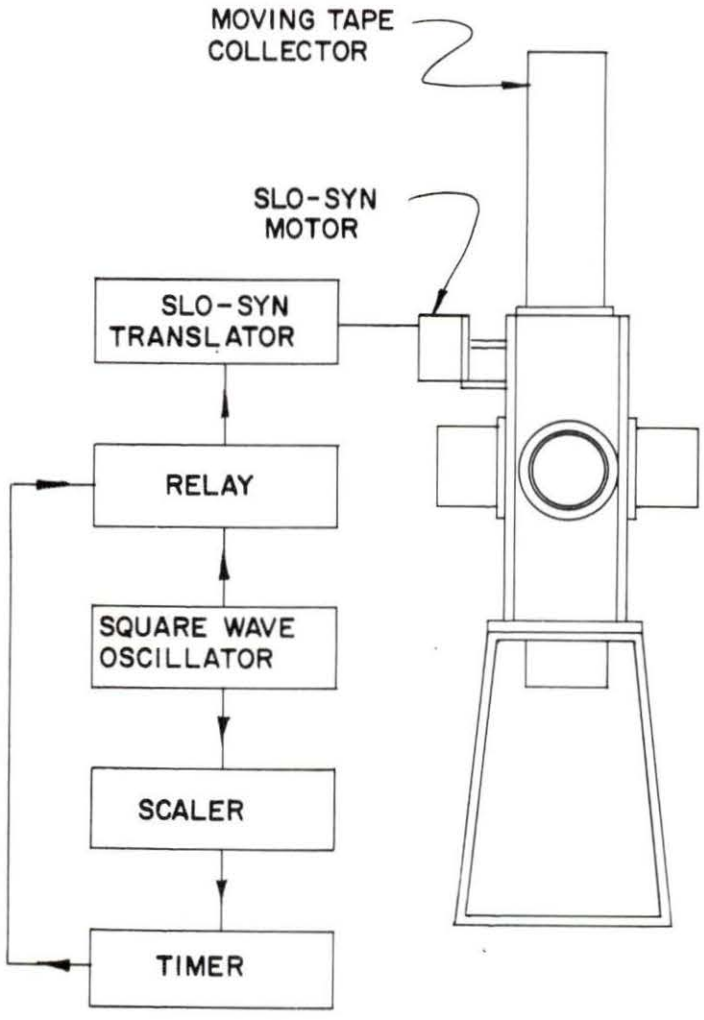

Figure 5. Experimental arrangement for measuring tape collector parameters

moved through the desired distance by operating the timer in the manual mode. Thus the required number of input pulses to exactly position the tape mark at some selected final position (i.e., the centerline of detector position 2) was recorded on the scaler.

The total number of steps (input pulses) supplied to the motor can be directly converted to distance in inches if the motor constant, C = 200 steps/revolution, and the actual diameter of the capstan, D, are known. Several capstan diameter measurements were made and a value of D = 1.013 $\pm$ 0.001 inches was obtained. Thus, the proportionality constant relating number of steps to distance is K = 62.85 $\pm$ 0.06 steps/inch. Actually, when using the tape collector, it is more convenient to express distances in steps rather than inches since the number of steps can be observed directly. For this reason, the tape collector constants were measured (using the procedure described above) and all distances were expressed in steps. Table 1 gives a list of the measured tape collector constants for each of the three aperture control configurations.

Table 1. Measured moving tape collector constants for three configurations of the aperture control at detector position 2

Number of passes at detector position 2	D_2	D_3	$a_1=a_2=a_3$	$(a_2)_{eff}$
1	517	1281	47	47
3	517	1427	47	204
5	517	1583	47	336

Finally, the ion beam height, h, is taken to be a nominal 0.75 inches. The height of the beam actually varies somewhat with the focus of the ion beam and is dependent upon day-to-day operation of the separator. This is probably the most uncertain parameter in the system, and it is not possible to satisfactorily determine a probable variation which would be realistic.

Tape collector equations

Using the measured parameters from above, with the aperture control device set to the maximum effective opening, Equations 19 through 24 were expressed as a function of motor input frequency, F, and are presented in Table 2.

Table 2. Tape collector equations for detector 2 aperture control set to the maximum effective opening (five pass arrangement)

Variable	Functional Relationship	Units
V	(0.0159) F	inches/second
T	(47.13)/F	seconds
$(\tau_d)_1$	0	seconds
$(\tau_d)_2$	(470)/F	seconds
$(\tau_d)_3$	(1536)/F	seconds
$(\tau_c)_1$	(47)/F	seconds
$(\tau_c)_2$	(336)/F	seconds
$(\tau_c)_3$	(47)/F	seconds

The variables, $(\tau_d)_3$, and $(\tau_c)_2$ are the only ones directly affected

by the aperture control device setting. Table 3 gives the equation for each variable as a function of F for each of the three possible aperture settings.

Table 3. $(\tau_d)_3$ and $(\tau_c)_2$ relationships for the three possible aperture control settings

Number of passes at detector position 2	Equation for $(\tau_d)_3$	Equation for $(\tau_c)_2$
1	(1234)/F	(47)/F
3	(1380)/F	(204)/F
5	(1536)/F	(336)/F

The relationships presented in Tables 2 and 3 thus can be used to calculate the motor speed, F, necessary to duplicate the times T, τ_d, and τ_c provided by the optimization program results for the particular tape collector configuration desired.

Mechanical Performance

The measurements of the mechanical performance were accomplished in three phases. First, the torque requirements of the moving tape collector were measured and compared with the observed motor torque. Second, the tape was operated discontinuously and moved over measured distances to determine the positioning accuracy for various transport times. Finally, the tape was operated continuously at various speeds and the measured tape speed was observed and compared with the predicted speed.

Torque measurements

The torque required to move the tape transport mechanism was measured by removing the motor coupling and attaching a lever to the rotary-motion vacuum feed-through shaft. A previously calibrated torque wrench was attached to the shaft and the torque necessary to move the tape for each of the three effective apertures at position 2 was measured. The five-pass arrangement required the largest torque which was observed to be 12.2 ounce-inches.

Next, the torque required to stall the motor was measured and found to be 53.2 ounce-inches or 41 ounce-inches in excess of the maximum load requirements. Thus the load imposed by the tape transport mechanism is well below the motor performance capabilities and it was observed that the angular velocity of the capstan was directly proportional to the motor drive input pulse frequency over the range from ~ 1 to 200 steps per second which includes the required range of speeds.

Discontinuous operation

The experimental setup shown in Figure 5 was again employed to determine the positioning accuracy of the tape transport system. In order to determine whether the positioning accuracy was dependent on motor input frequency, the tape was transported over previously measured distances at various speeds. For these measurements the desired number of steps corresponding to the measured length was preset on the scaler unit, the tape mark was positioned at the initial point, a tape speed was selected by adjusting the pulse rate to the desired value, and the timer was started. After the tape stopped automatically when the preselected number of steps

was reached, the tape mark was observed for deviation from the desired final position by comparing its position with a similar mark on the main body of the tape collector.

Measurements were made at transport speeds over the range from ~1 step per second to ~100 steps per second for three different distances; from detector 1-B centerline to detector 2 centerline (D_2), from detector 1-B centerline to detector 3 centerline (D_3), and from detector 2 centerline to detector 3 centerline (D_3-D_2). The total time and number of steps were recorded for each measurement.

The largest error observed was an error of 1/64 inch over a distance of 8.226 inches or a percent error of 0.19%. The error was observed to be not frequency dependent. The mean error for all measurements was $\pm$0.04%. Thus the observed positioning error was for all practical purposes negligible.

Continuous operation

The previously described experimental arrangement was used to measure the tape speed under conditions of continuous operation except that the relay was removed. The drive unit was thus able to run continuously and was not controlled by the timer.

The tape speed was measured by determining the time required for the tape to traverse a known distance. The measurement technique required manual operation of the timer as an appropriately placed mark on the tape passed over the measured distance.

Tape speeds were measured over the range from ~1 step per second to ~300 steps per second for each of the three aperture control

configurations at detector position 2. The largest observed error (relative to the calculated theoretical speed) was 1.30% and the mean error was 0.44% with a standard deviation of $\pm$0.61%. Thus, the average observed speed was 0.44% greater than the theoretical speed. It is likely that the above results were biased by the manual timer operation required for this measurement since from the previous discontinuous measurements there was no evidence for errors of the magnitude obtained here.

Cross Detection Characteristics

The cross detection characteristics were measured by mounting a gamma-ray source on the collector tape and recording the activity measured by a NaI(Tl) detector located in a detector station as the tape was driven through a cycle.

Since the metalized coating on the tape is composed of a cobalt and nickel alloy, a small piece was irradiated in the reactor and used as a convenient source. The irradiated tape was set aside until only the Co^{60} activity remained and then it was simply spliced into a continuous loop of tape mounted in the tape collector. The source size was chosen to approximate the area of activity deposited by a well focused ion beam.

The NaI(Tl) detector was mounted at a detector station and shielded from room background by 4 inches of lead bricks stacked exterior to the tape collector. All interior lead shielding was installed and the tape collector was placed in normal operating condition. The output from the NaI(Tl) detector was amplified and fed into a Nuclear Data 128 channel pulse-height analyzer, used in a multiscaling mode. The amplifier discriminator was adjusted to cut off the Co^{60} spectrum just below the 1.33

MeV peak.

For a typical measurement the source was positioned at the centerline of detector station 1-B to simulate the deposit of activity by the isotope separator and the NaI(Tl) crystal was placed in the detector station to be tested. The analyzer dwell time was set to 1 second per channel. The tape speed was set to make one complete circuit in 128 seconds. The analyzer and tape transport system were then started simultaneously and stopped at the completion of one cycle. The analyzer output provided a display of the observed activity at the detector location as a function of source position in the tape collector.

The initial cross detection measurements at detector stations 1-B and 2 demonstrated that the internal shielding was not adequate in the areas between detectors. Measurements were discontinued and additional lead shielding was fabricated and installed wherever possible.

A complete set of measurements was made after the modified shielding was installed and the results appear in Figure 6. The graph shows the cross detection characteristics for each detector station. From the graph it is observed that the cross detection between detector station centerlines is a maximum of about 2%.

It is important to note that these measurements were made with an essentially constant activity source whereas in actual operation rapidly decaying, short-lived sources are deposited on the tape and the cross detection obtained is a function of whether the source is up stream or down stream from the detector in question. For example, if a detector is located at position 1-B, the tape is operated in the continuous mode, and the ion beam is continuously deposited, the cross detection from tape

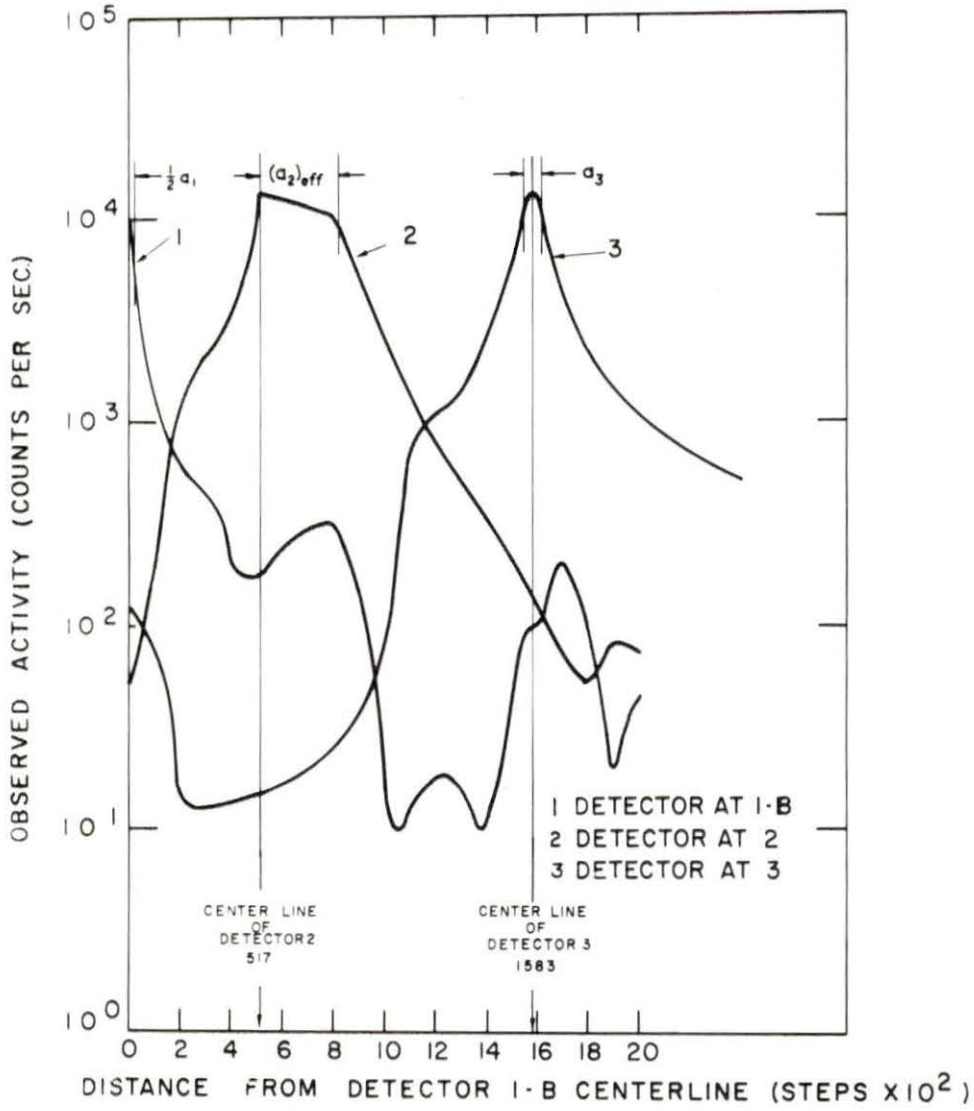

Figure 6. Cross detection characteristics for detectors 1-B, 2, and 3

deposited activity located at the centerline of detector 2 will be less than the maximum 2% value due to the decay of activity during transit. A completely different situation exists when a detector is located at position 2 and consideration is given to the cross detection from activity being continuously deposited at detector position 1. It is quite possible that the total activity deposited at detector 1 is a factor of 100 greater than the total activity observed at detector 2 due again to the activity decay in transit. Thus, in this case, even though the cross detection factor from detector 1 is observed from Figure 6 to be $\sim 0.5\%$, fully half the total activity observed at detector 2 would consist of cross detection from the beam deposit point. The results of Figure 6 should thus be used with caution when evaluating the cross detection properties of down stream detectors.

When the tape collector is operated in a discontinuous mode (i.e., the activity is collected for a period of time, T, allowed to decay for a time, τ_d, observed for a time, τ_c, and then the active portion of the tape is moved away to prepare for another cycle) it is possible to take advantage of the particularly well shielded areas of the tape collector. The best shielding occurs at the valleys of the curves on Figure 6. Thus, when detector position 1 is used for activity observation in the discontinuous mode the active portion of the tape should be moved a total of 1050 steps after the detection period. At that position cross detection at detector 1 will be less than $\sim 0.1\%$.

Finally, it should be noted that the cross detection measurements for detector position 2 were performed for the maximum effective aperture. The drop in count rate across the aperture is a geometry effect caused by

the tape moving further away from the detector with each successive pass. (Figure 4 shows the mechanism involved.)

DISCUSSION OF ANALYTICAL RESULTS

The results of the preceeding section demonstrated that the moving tape collector was capable of translating the times required by the optimization procedure into tape speed with little appreciable error. Also, the internal shielding was shown to be adequate to insure that no more than 2% cross detection is present in most cases.

This section presents a discussion of the ion beam characteristics that affect the activity deposition at the moving tape collector, the results of the optimization program, and some observed results.

Ion Beam Characteristics

The present source installed in the TRISTAN system is designed to release gaseous fission products. Thus, only Br, Kr, I, and Xe are released to any appreciable extent by the source. Furthermore, the transport line from the fission source and the isotope separator ion source tend to trap out the chemically active gasses Br and I so that only the noble gasses Kr and Xe are present to any measurable extent in the ion beam from the separator. This feature of the TRISTAN system assures that the parent activity deposited at the moving tape collector will be either a Kr or Xe isotope.

Another property of the ion beam that effects the input parameters to the optimization program is called the cross contamination effect. When an isotope separator beam is focused on a particular mass number the beam exhibits a certain amount of dispersion. If the dispersion is large then an appreciable percentage of the mass number selected will appear at the position of the next higher or lower mass number. Cross contamination is

thus a measure of the amount of activity of mass, A, appearing in the mass $A \pm 1$ position when the isotope separator beam is focused on mass A.

The cross contamination of the TRISTAN beam was measured in the following manner. The isotope separator was focused on singly ionized mass 85 and the fission source was used to produce the 4.5 hour Kr^{85m} isotope. For this measurement the normal 0.09375 inch beam defining slit was removed and a row of heavy duty office staples was mounted at the focal surface of the ion beam in the collector box (see Figure 1) so that the radioactive Kr^{85m} was deposited directly on the staples. After sufficient activity had been deposited the staples were removed from the collector box, separated, and counted in pairs with a Ge(Li) detector to count the 150 keV gamma ray in the decay of Kr^{85m}. The results are shown in Figure 7. This curve is also representative of cross contamination at other mass numbers. The peak shown at the next higher mass number is caused by hydride formation with mass 85 and the dotted line indicates the expected level after the hydride problem has been eliminated. Also shown about the peak is the width of the normal beam defining slit located in the collector box. From the curve it is observed that under normal conditions the cross contamination will be less than a factor of 5×10^{-5} and thus it is reasonable to neglect the presence of other mass numbers in the beam.

It should be noted, however, that cross contamination from the next lower mass number will in general be more significant than that of the next higher mass when using a fission source to produce radioactive nuclides. The reason for this effect is that as the mass number of a particular isotope increases the fission yield decreases. Thus, as the isotopes move away from the stability line, the fission yield for a particular mass

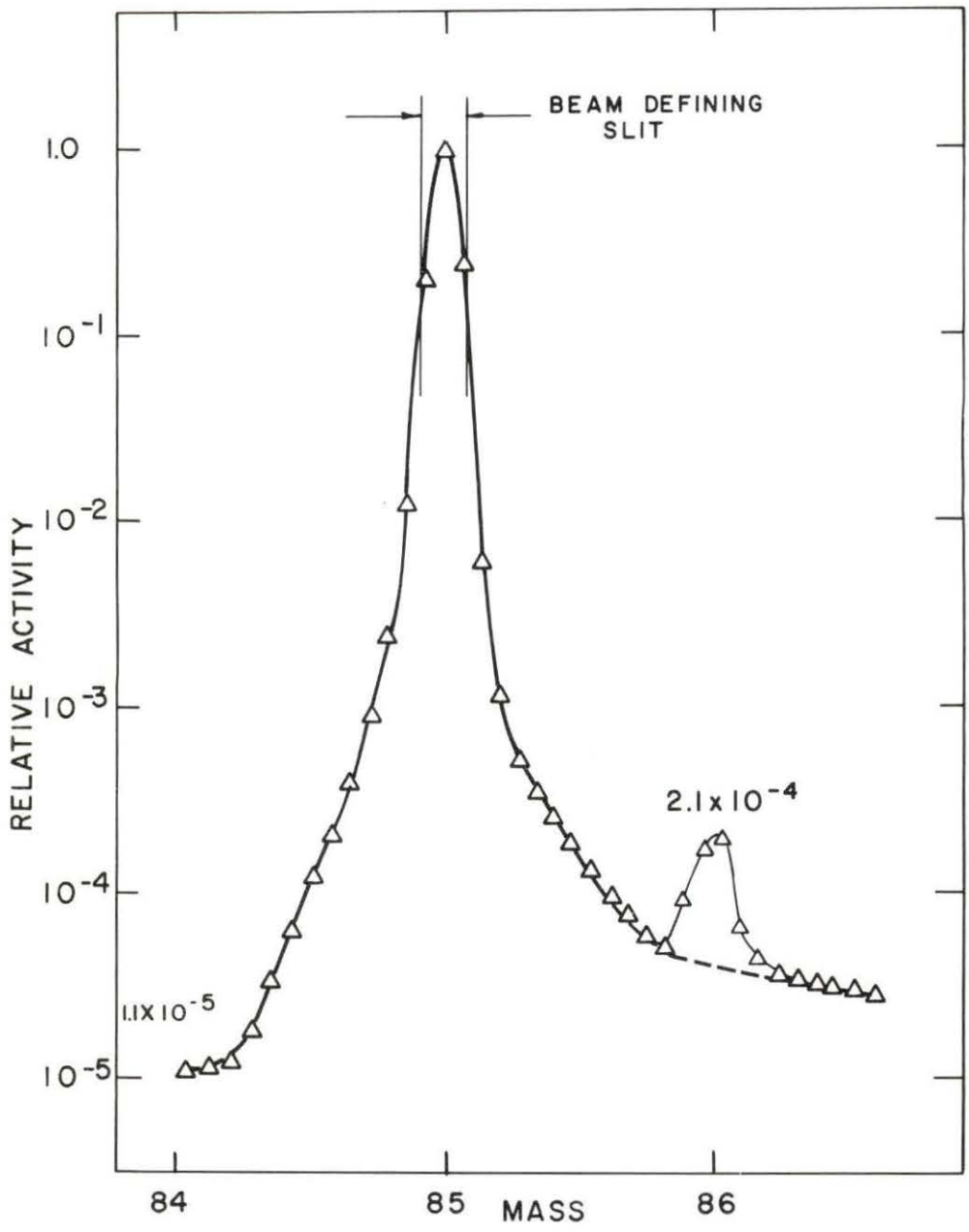

Figure 7. Cross contamination at ion beam focal surface for singly ionized mass 85

number, A, according to Wahl, et al. (10), can be as much as a factor of 10 less than mass A-1 thereby increasing the cross contamination from the lower mass to about 5×10^{-4}. Furthermore, decay differences of adjacent short-lived mass numbers while in transit to the ion source can enhance the lower mass number activity by a factor of up to 100 depending on half-life differences. As these effects may be significant in some experiments, due consideration should be given to the relative fission yields and half-lives of adjacent mass numbers to estimate the magnitude of cross contamination.

In summary, the present TRISTAN system produces an ion beam that closely approximates the simple buildup and decay scheme in which P_1 is the only non zero production term.

General Results of Optimization Procedure

The ISOBAR and ISOMAX programs were run to determine the maximum attainable activity separation for each member of the decay chains capable of being produced by the TRISTAN source. The ISOBAR program was run first to provide the initial estimates for the optimization procedure in the ISOMAX program.

It should be noted that the optimization procedure was not applied to the first and last members of a decay chain since these represent trivial cases. Thus, for the first member of a decay chain the activity ratio is a maximum when the beam of parent atoms is initially deposited and becomes continually smaller as the daughter products build up. Hence, to maximize the activity separation of the first member the tape should be run continuously and as rapidly as acceptable counting statistics will allow.

The activity separation of the first member of each decay chain is calculated for various tape speeds and printed out by program ISOMAX.

The last member of a decay chain can obviously be separated by simply waiting until all other parent activities have decayed to negligible levels. An exception to this rule occurs when the last member of the decay chain has a shorter half-life than its parent. Then it must be studied in equilibrium with the parent activity.

For decay chains with three or more members the activity ratio of the middle members exhibits a unique maximum for some collection time, T, and delay time, τ_d. Table 4 presents the results of the optimization procedure. Included in the table are the isotope half-life from Lederer et al. (6), the optimization times T and τ_d, the activity separation ratio, and the fraction of saturated activity. The first member of the decay chain is also listed and the motor speed required to produce a 0.95 or better separation factor is given. If the 0.95 factor is not attainable the speed for the next best separation factor is given.

From a practical standpoint the data presented in Table 4 have a serious limitation since, as a general rule, the maximum of the activity ratio occurs in a low saturated activity region. Thus, the saturated activity is often in the 0.01 to 0.05 range when the activity ratio is maximized. The results thus have limited value in determining the optimum collect and delay times for practical problems.

A more satisfactory approach makes use of program ISOBAR and particularly the output of subroutine CALTAB. Recall that the 10 by 20 output array contains values of activity ratio and fractional saturated activities. With a simple visual inspection of the output, the best possible

Table 4. Results of optimization program ISOMAX for Kr^{89} to Kr^{95} and Xe^{139} to Xe^{143}

Decay chain identification	Decay chain member	Half-life (seconds)	Collect time (seconds)	Delay time (seconds)	Motor speed (steps/sec)	Maximum activity ratio	Fraction of saturated activity
Kr^{89}	Kr^{89}	192			1.47	0.9880	0.1091
	Rb^{89}	924	378	2964		0.9980	0.0337
Kr^{90}	Kr^{90}	33			2.08	0.9550	0.3782
	Rb^{90}	174	309	978		1.0000	0.0177
	Sr^{90}	8.861×10^8	8.8×10^7	8.8×10^7		0.5000	0.0621
Kr^{91}	Kr^{91}	10			5.9	0.9607	0.4256
	Rb^{91}	72	29.13	132.9		0.9937	0.0790
	Sr^{91}	3.481×10^4	3.48×10^3	1×10^3		0.9985	0.0659
Kr^{92}	Kr^{92}	1.86			47.1	0.9377	0.3111
	Rb^{92}	5.3	5.3	29.8		0.9762	0.0156
	Sr^{92}	9.756×10^3	497	123		0.9807	0.0344
Kr^{93}	Kr^{93}	2			47.1	0.9409	0.2929
	Rb^{93}	5.6	0.61	17.7		0.9162	0.0124
	Sr^{93}	480	48	85		0.9974	0.0602
Kr^{94}	Kr^{94}	1.4			66.7	0.9220	0.2953
	Rb^{94}	2.9	0.83	8.53		0.7950	0.0407
	Sr^{94}	78	6.88	38.4		0.9736	0.0446
Kr^{95}	Kr^{95}	0.1			66.7	0.8728	0.9926
	Rb^{95}	2.5	0.1	1.41		0.9770	0.1996
	Sr^{95}	48	4.01	29.2		0.9611	0.0390
	Y^{95}	654	368	1.16×10^3		0.9997	0.1023

Table 4. (continued)

Decay chain identification	Decay chain member	Half-life (seconds)	Collect time (seconds)	Delay time (seconds)	Motor speed (steps/sec)	Maximum activity ratio	Fraction of saturated activity
Xe^{139}	Xe^{139}	43			1.04	0.9706	0.5178
	Cs^{139}	570	247	341		0.9168	0.1850
Xe^{140}	Xe^{140}	16			4.17	0.9419	0.3874
	Cs^{140}	66	3.71	371		0.9978	0.0010
	Ba^{140}	1.106×10^6	2×10^5	600		0.7220	0.1177
Xe^{141}	Xe^{141}	2			16.7	0.9560	0.6247
	Cs^{141}	24	2.4	24		0.9769	0.0365
	Ba^{141}	1.08×10^3	19.2	342		0.9810	0.0101
	La^{141}	1.404×10^4	4.44×10^3	1.4×10^4		0.9937	0.1070
Xe^{142}	Xe^{142}	1.5			66.7	0.9053	0.2787
	Cs^{142}	2.3	1.194	11.85		0.8776	0.0211
	Ba^{142}	660	6.48	45.23		0.9941	0.0065
Xe^{143}	Xe^{143}	1			66.7	0.8900	0.3874
	Cs^{143}	2	1.99	3.72		0.6412	0.2177
	Ba^{143}	12	3.07	22.92		0.9630	0.0565
	La^{143}	840	154	203.8		0.9982	0.1028
	Ce^{143}	1.188×10^5	6.68×10^3	1.19×10^4		0.9900	0.0359

activity separation for some minimum acceptable fraction of saturated activity can be found. The next section shows how this technique was applied to the Kr^{92} chain.

Actual Optimization Parameters for the Kr^{92} Chain

Since the half-lives of Kr^{92} and Rb^{92} are fairly close together relative to the longer lived Sr^{92}, the main problem was the activity separation of the first two members of the decay chain. Both continuous and discontinuous tape collector operation were investigated and compared to determine the best method of separation.

Clearly, continuous operation must be used to efficiently separate Kr^{92} at detector position 1. A calculation was made assuming that a detector was also located at position 2 to determine if a simultaneous separation of Rb^{92} would be possible. The calculation was made for various continuous tape speeds and the plotted results appear on Figure 8. From the curve it is observed that at a motor speed of 25 steps per second a simultaneous separation of about 0.90 should be obtained for Kr^{92} at detector 1 and Rb^{92} at detector 2. A careful consideration of the activity levels involved and the internal shielding arrangement indicates that such a scheme is not practical. At the 25 steps/second speed, the Kr^{92} activity is $\sim$ 20% saturated and Rb^{92} activity at detector 2 is only $\sim$ 0.2% saturated. Thus, the total activity at detector 1 is approximately a factor of 100 times the total activity at detector 2. Since the cross detection at detector 2 is about 0.5%, then it is likely that half of the activity detected at detector 2 will be cross detection from the activity deposited at detector 1. On this basis, simultaneous activity separation

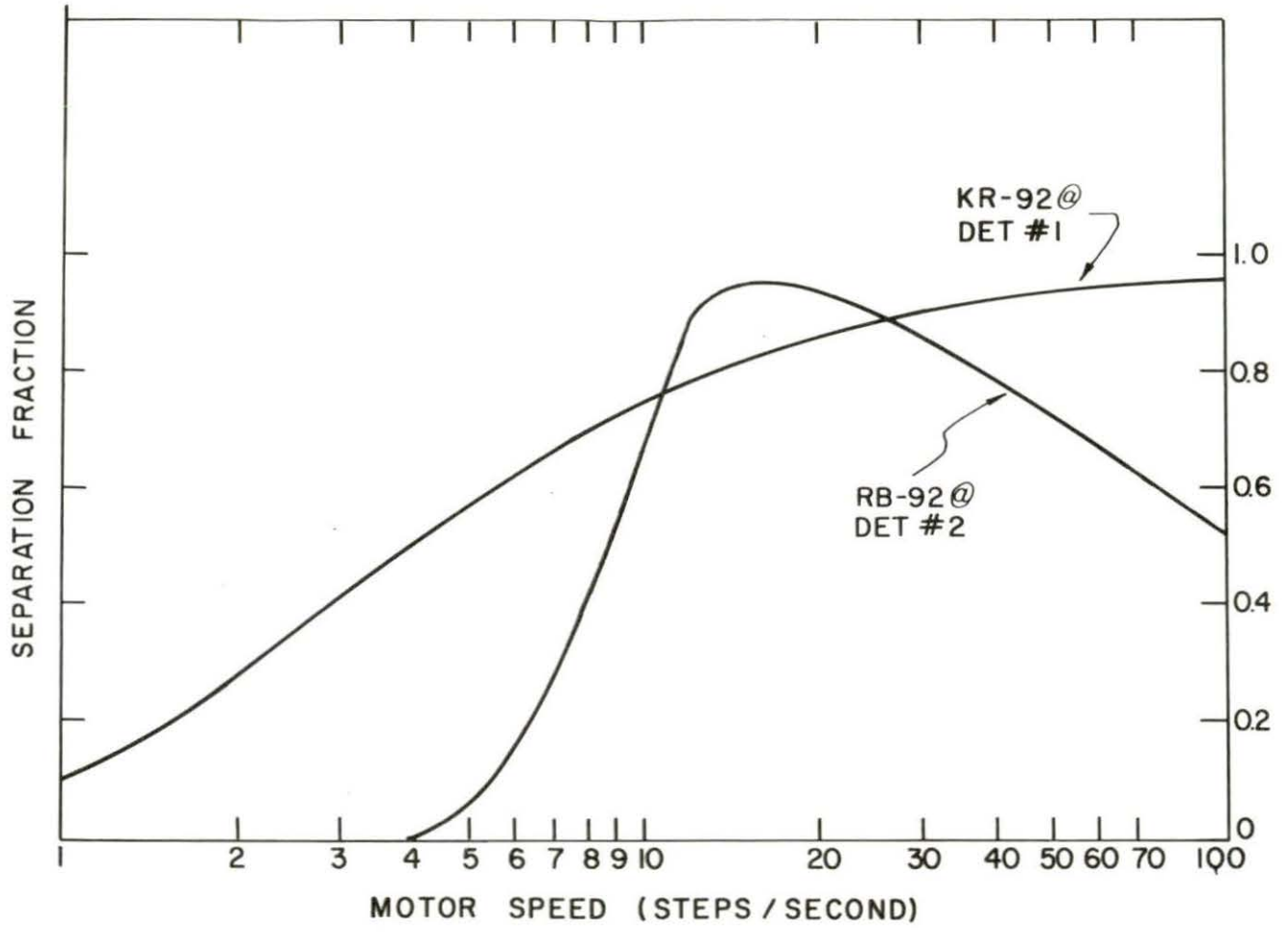

Figure 8. Predicted simultaneous separation ratios at detectors 1 and 2 as a function of tape speed

at two different detectors was rejected for mass 92.

Next, program ISOBAR was used to determine the optimum times for separating Rb^{92} with a discontinuous tape operation. From the CALTAB output it was found that for T = 30 seconds, τ_d = 9 seconds, and τ_c = 9 seconds a separation of 0.9540 with a 0.3104 saturation factor was predicted. An experiment is currently in progress using these optimized times, with acceptable separation and count rate.

The results of an earlier experiment on mass 92 is shown in Figure 9. The upper half of the figure shows a gamma-ray spectrum that contains components of the decays of both Kr^{92} and Rb^{92}. Particularly prominent is the 150 keV peak from Kr^{92} decay. The lower half shows the effect of discontinuous tape operation in which a delay time of 11 seconds has been employed after the collection period. Note that all gamma-ray peaks from the decay of Kr^{92} have disappeared except for the 150 keV peak and it is greatly diminished. Equally important is the fact that the peaks from the decay of Rb^{92} are noticeably enhanced.

Finally, it is noted from the output of CALTAB that the value of $R_i(T,\tau_d)$ in the region near its maximum is in general rather broad and flat and the maximum value is not very sensitive to small changes in T and τ_d. Thus, a measure of freedom is allowable in the choice of the actual collection and delay times.

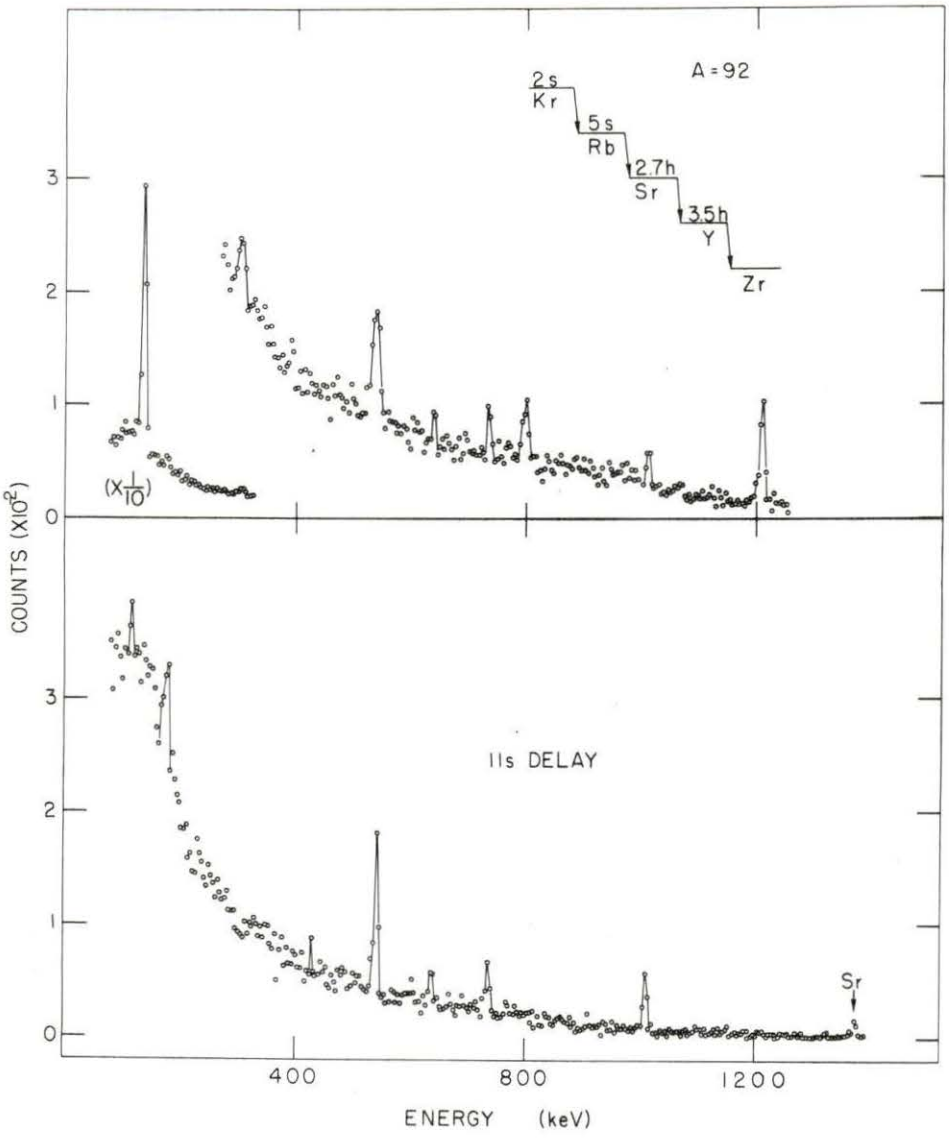

Figure 9. Effect of delay on second member separation

CONCLUSIONS

The moving tape collector installed in the TRISTAN system has been demonstrated to be capable of separating the activity of decay chain members by both continuous and discontinuous operation. Figure 10, for example, shows some typical results for the mass 91 decay chain. The upper curve corresponds to a continuous tape operation mode for the separation of the first member of a decay chain and it is essentially a pure Kr^{91} spectrum with a small Rb^{91} peak at ~500 keV. The middle curve corresponds to a discontinuous tape operation for the separation of a second member and the spectrum is observed to be a relatively pure Rb^{91} spectrum with a small Sr^{91} peak at ~325 keV. The lower curve shows the equilibrium activity of the chain for comparison purposes.

The tape transport characteristics were found to be excellent. The cross detection properties were found to be adequate for most applications except for the problem of downstream cross detection mentioned previously.

The overall cross detection properties could be improved somewhat by replacing the present lead shielding with a higher atomic number material such as tungsten or canned depleted uranium. A redesigned device should provide for a minimum of 4 inches of lead or its equivalent between every part of the tape and all areas of the detectors. Also, consideration should be given to eliminating detector position 3 and designing detector position 2 so that the distance between it and the beam deposit point could be varied. This arrangement, coupled with a well shielded beam deposit point, might make it feasible to separate two decay chain member activities simultaneously as noted before. Finally, for the discontinuous type

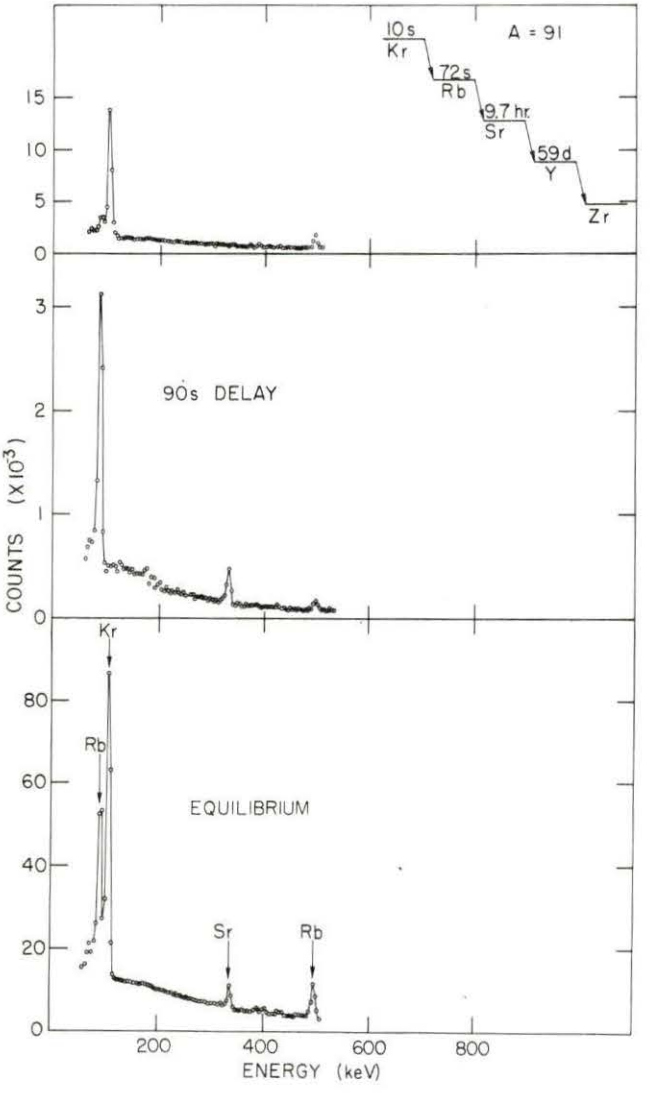

Figure 10. Activity separation for mass 91

measurements, a position should be supplied (preferably as close as possible to the deposit point to conserve tape) that gives a gamma attenuation of from 10^5 to 10^6 for storing the radioactive portion of the tape after a measurement cycle.

The analytical technique employed provides a general solution for the buildup and decay of multiple production term decay chains. The application of program ISOBAR to the solution of single production decay chains coupled with the subroutine CALTAB provided a convenient, visual method of selecting the optimum activity separation and appropriate saturated activity fraction to yield an adequate count rate of the activity desired. The less preferred ISOMAX program optimized only the activity ratio and thus could not provide assurance of an adequate count rate.

Finally, the application of this work to the solution of the more complicated multiproduction term decay chains will be useful in future work in which the halogen fission products will be extracted in conjunction with the noble gasses.

BIBLIOGRAPHY

1. Alvager, T., Naumann, R. A., Petry, R. F., Sidenius, G., and Thomas, T. Darrah. On-line studies of mass-separated xenon fission products. Physical Review 167: 1105-1116. 1968.

2. Bateman, H. The solution of differential equations occurring in the theory of radio-active transformations. Cambridge Philosophical Society Proceedings 15: 423-427. 1910.

3. Borg, S., Fagerquist, U., Holm, G., and Kropff, F. Isotope separator on-line studies of gaseous fission products. Arkiv for Fysik 34: 413-432. 1967.

4. Crancon, J. and Moussa, A. A study of short-lived fission products by means of an isotope separator connected to a reactor. U.S. Atomic Energy Commission Report UCRL-Trans-10130 (California. University, Berkeley. Radiation Lab.). 1967.

5. Day, G. M., Tucker, A. B., and Talbert, W. L., Jr. Preliminary studies of delayed neutron emission from separated isotopes of gaseous fission products. U.S. Atomic Energy Commission Report IS-1567 (Iowa State University of Science and Technology, Ames. Institute for Atomic Research). 1967.

6. Lederer, C. M., Hollander, J. M., and Perlman, I. Table of isotopes. 6th ed. New York, N.Y., John Wiley and Sons, Inc. 1967.

7. McElhone, D. H. A matrix formulation of steepest ascent methods for optimization problems. Unpublished M.A. thesis. Austin, Texas, Library, The University of Texas. 1965.

8. Sidenius, G., Gammon, R. M., Naumann, R. A., and Thomas, T. D. On-line separation of short-lived products from ^{252}Cf spontaneous fission. Nuclear Instrumentation Methods 38: 299-302. 1965.

9. Talbert, W. L., Jr. and McConnell, J. R. Preparation for on-line studies of short-lived nuclei produced by a reactor. Arkiv for Fysik 36: 99-105. 1967.

10. Wahl, A. C., Ferguson, R. L., Nethway, D. R., Troutner, D. E., and Wolfsberg, Z. K. Nuclear-charge distribution in low-energy fission. Physical Review 126: 1112-1127. 1962.

ACKNOWLEDGMENTS

The author acknowledges his indebtedness to the late George M. Day for the suggestion of this problem.

Acknowledgment should also be made for the efforts of R. G. Struss and F. D. Michaud in the design and construction of the moving tape collector.

Finally, acknowledgment is made for the help received from the Computer Services Group, for the inspiration provided by Dr. W. L. Talbert, and for the patience demonstrated by Dr. Donald M. Roberts.

APPENDIX A

Program ISOBAR Description and Flow Chart

This section presents the description, flow chart, and program listing for the ISOBAR main program and subroutines.

The flow chart for the ISOBAR main program is given in Figure 11. The input and output parameters are defined as follows:

MEMI - Alphameric name of first member of decay chain

L - Number of production terms

N - Number of members in the decay chain

MEMBR - Alphameric array of decay chain member names

THALF - Array of decay chain member half-lives

P - Array of production term values

T - Collect or buildup time

TAUD - Delay or decay time

TAUC - Count time

A - Array of calculated activities

D - Array of calculated integrated activities

PCT - Array of calculated percent saturation values

RNEW - Array of calculated activity ratios

SNEW - Array of calculated integrated activity ratios

As indicated on the flow chart the main program reads and stores the input data, calculates the value of the activity and activity ratio of all members of a decay chain for each value of T, TAUD, and TAUC read in, and prints out the data in a suitable format.

The main program calls three subroutines RATIO, DATIO, and CALTAB.

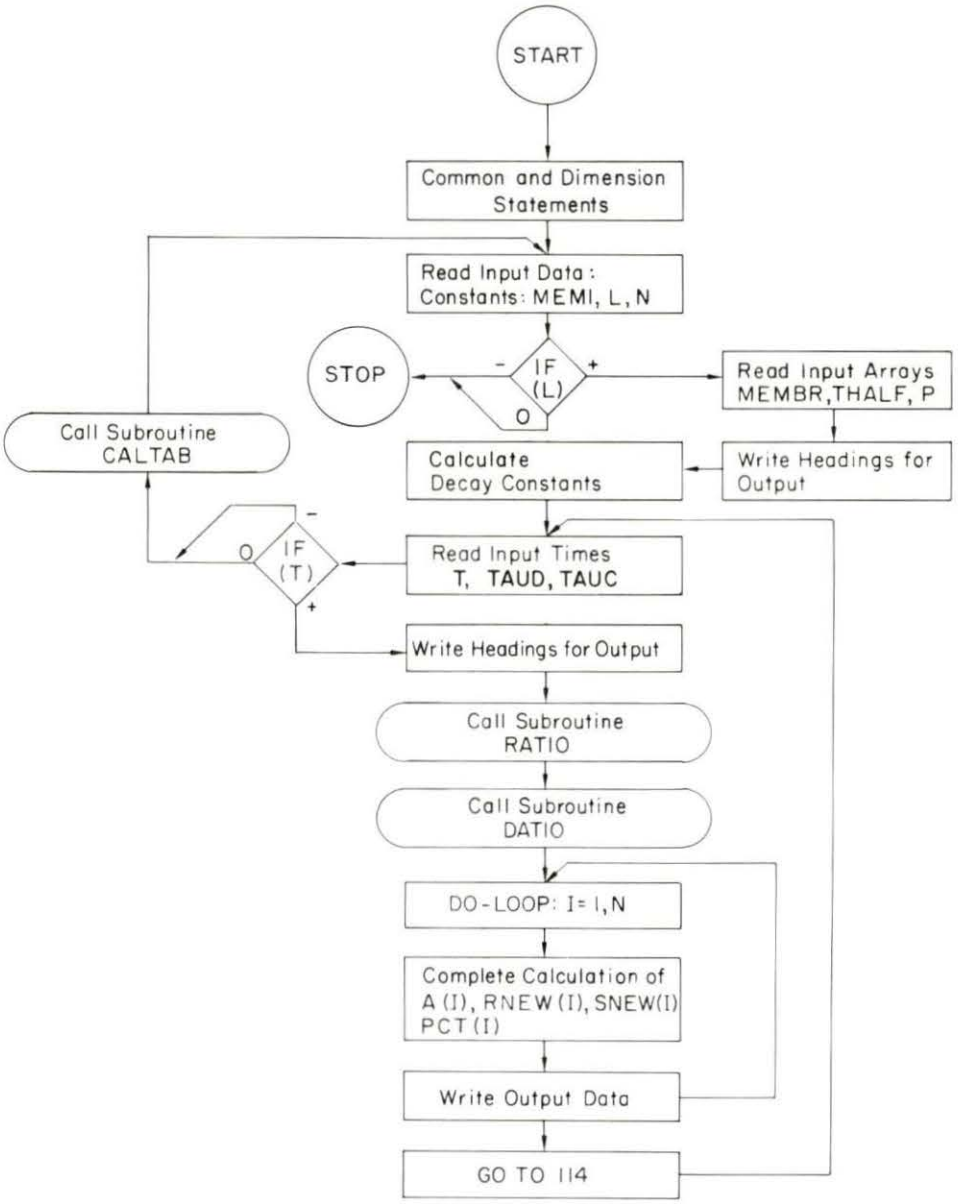

Figure 11. Flow chart for ISOBAR main program

Subroutine RATIO calculates the value of $A_i(T,\tau_d)$ as given by Equation 12 for each decay chain member using the current values of T and τ_d supplied by the main program. RATIO calls two additional subroutines, PRDCT and SUMMTN. PRDCT calculates the denominator of Equation 12 and SUMMTN calculates the series of multiplied decay constants and production terms preceding the second summation of Equation 12. Figure 12 gives the flow chart for subroutines RATIO, PRDCT, and SUMMTN.

Subroutine DATIO calculates the value of $D_i(T,\tau_d,\tau_c)$ as given by Equation 15 for each decay chain member using the main program supplied values of T, τ_d, and τ_c. The subroutine is very similar to RATIO and the flow chart is not included.

Subroutine CALTAB shown in Figure 13 calculates a matrix of values of $A_i(T,\tau_d)$ and saturated activity fraction and prints out the results in a suitable format. The calculations cover the range THALF(I)/1000 $\leq$ T $\leq$ 10 THALF(I) and THALF(I)/10 $\leq$ TAUD $\leq$ 10 THALF(I). The print out is a 10 by 20 array with the variable, T, assigned 20 values and the variable, TAUD, assigned 10 values.

The program listing of ISOBAR and its called subroutines appears on pages 54 through 60.

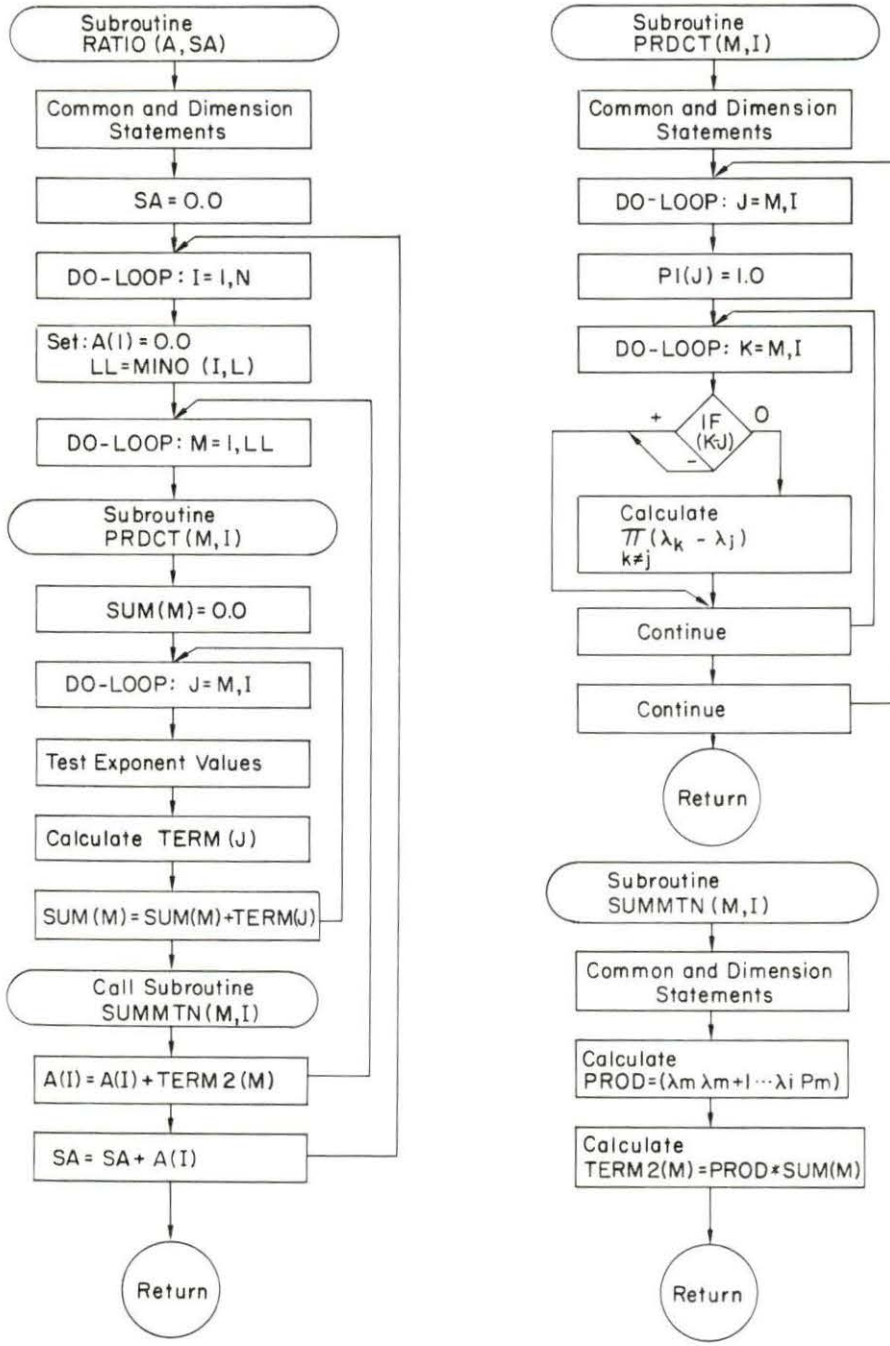

Figure 12. Flow chart for subroutines RATIO, PRDCT, SUMMTN

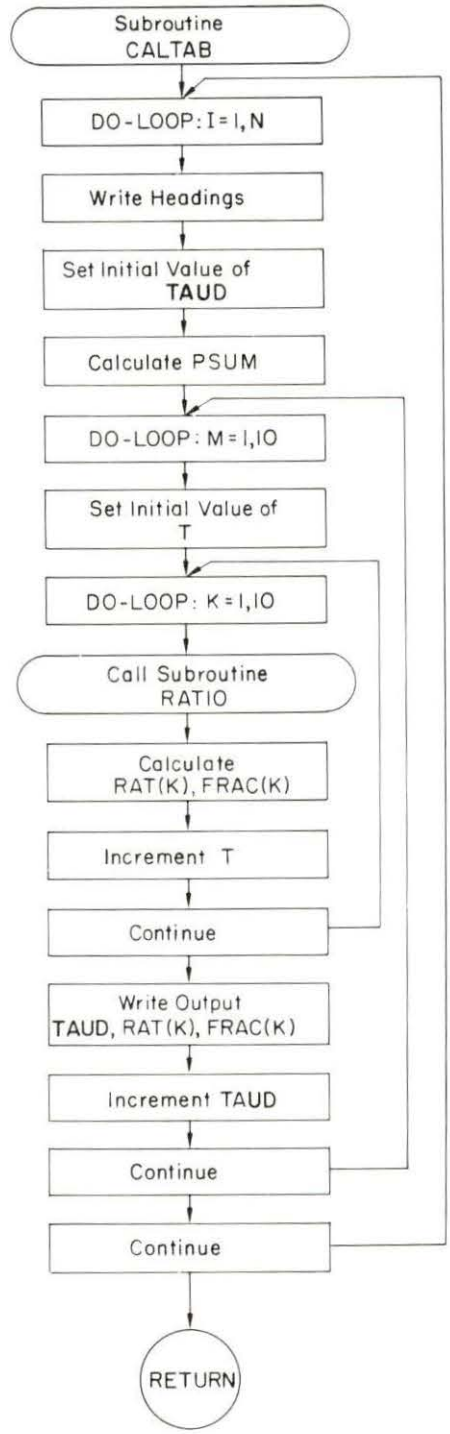

Figure 13. Flow chart for subroutine CALTAB

```
C
C
C  --ISOBAR--- A PROGRAM FOR CALCULATING ACTIVITY SEPARATION
C                              IN DECAY CHAINS
C
C
      COMMON RAT(10),TEE(10),FRAC(10),DECAY(8),THALF(8),P(8),
     1PI(8),SUM(8),TERM(8),TERM2(8),MEMBR(8),T,TAUD,TAUC,N,L,
     1II
      DOUBLE PRECISION DECAY,THALF,P,PI,SUM,TERM,TERM2,T,TAUD,
     1TAUC,MEMBR,PCT(8),A(8),D(8),MEM1,RNEW(8),SNEW(8),SA,SD,
     1DEXP,DABS,PSUM,RAT,TEE,PROD,FRAC
   13 READ(1,10001)MEM1,L,N
10001 FORMAT(A8,2I3)
      IF(L)115,115,116
  116 READ(1,1001) (MEMBR(J),J=1,N)
 1001 FORMAT(8A8)
      READ(1,10002)(THALF(I),I=1,N)
      READ(1,10002)(P(I),I=1,L)
10002 FORMAT(4D20.12)
      WRITE(3,1002)MEM1,L
 1002 FORMAT(@1    CHAIN @,A8,@  WITH @,I1,
     1@ PRODUCTION TERM(S)@,/)
      WRITE(3,104)
  104 FORMAT(@           PRODUCTION TERM      PRODUCTION CONST@,
     1/)
      DO 105 I=1,L
  105 WRITE(3,106)I,P(I)
  106 FORMAT(12X,I1,15X,D20.12)
      DO 100 I=1,N
  100 DECAY(I)=0.69315/THALF(I)
  114 READ(1,107)T,TAUD,TAUC
  107 FORMAT(3D20.12)
      IF(T)108,108,109
  109 WRITE(3,110)T,TAUD,TAUC
  110 FORMAT(@0@,9X,@COLLECT TIME(T)=@,D16.8,@,  DELAY TIME@,
     1@(TAUD)=@,D16.8,@,       COUNT TIME(TAUC)=@,D16.8,/)
      WRITE(3,111)
  111 FORMAT(10X,@MEMBER     NAME      HALFLIFE(SEC)     ACT@,
     1@IVITY(D/S)   PERCENT SAT.    ACT.RATIO@,8X,@INT.@,
     1@RATIO@,/)
  112 FORMAT(13X,I1,5X,A8,3X,5D16.8)
      PSUM=0.D0
      CALL RATIO(A,SA)
      CALL RATIO(D,SD)
      DO 113 I=1,N
      IF(L-I)201,200,200
  200 PSUM=PSUM+P(I)
  201 RNEW(I)=A(I)/SA
      SNEW(I)=D(I)/SD
      PCT(I)=A(I)*100.D0/PSUM
```

```
113 WRITE(3,112)I,MEMBR(I),THALF(I),A(I),PCT(I),RNEW(I),
   1SNEW(I)
    GO TO 114
108 CALL CALTAB
    GO TO 13
115 STOP
    END
```

```
      SUBROUTINE RATIC (A,SA)
      COMMON RAT(10),TEE(10),FRAC(10),DECAY(8),THALF(8),P(8),
     1PI(8),SUM(8),TERM(8),TERM2(8),MEMBR(8),T,TAUD,TAUC,N,L,
     1II
      DOUBLE PRECISION DECAY,THALF,P,PI,SUM,TERM,TERM2,T,TAUD,
     1TAUC,MEMBR,PCT(8),A(8),D(8),MEM1,RNEW(8),SNEW(8),SA,SD,
     1DEXP,DABS,PSUM,RAT,TEE,PROD,FRAC
      SA =0.D0
      DO 400 I=1,N
      A(I)=0.D0
      LL=MIN0(I,L)
      DO 300 M=1,LL
      CALL PRDCT (M,I)
      SUM(M)=0.D0
      DO 200 J=M,I
      IF(DABS(DECAY(J)*T)-174.D0)500,600,600
  500 IF(DABS(DECAY(J)*TAUD)-174.D0)700,900,900
  600 IF(DABS(DECAY(J)*TAUD)-174.D0)800,900,900
  900 TERM(J)=0.D0
      GO TO 200
  800 TERM(J)=DEXP(-DECAY(J)*TAUD)/(DECAY(J)*PI(J))
      GO TO 200
  700 TERM(J)=(1.0D0-DEXP(-DECAY(J)*T))*DEXP(-DECAY(J)*TAUD)/
     1   (DECAY(J)*PI(J))
  200 SUM(M)=SUM(M)+TERM(J)
      CALL SUMMTN (M,I)
  300 A(I)=A(I)+TERM2(M)
  400 SA=SA+A(I)
      RETURN
      END
```

```
      SUBROUTINE DATIO(D,SD)
      COMMON RAT(10),TEE(10),FRAC(10),DECAY(8),THALF(8),P(8),
     1PI(8),SUM(8),TERM(8),TERM2(8),MEMBR(8),T,TAUD,TAUC,N,L,
     1II
      DOUBLE PRECISION DECAY,THALF,P,PI,SUM,TERM,TERM2,T,TAUD,
     1TAUC,MEMBR,PCT(8),A(8),D(8),MEM1,RNEW(8),SNEW(8),SA,SD,
     1DEXP,DABS,PSUM,RAT,TEE,PROD,FRAC
      SD=0.D0
      DO 400 I=1,N
      D(I)=0.D0
      LL=MIN0(I,L)
      DO 300 M=1,LL
      CALL PRDCT(M,I)
      SUM(M)=0.D0
      DO 200 J=M,I
      IF(DABS(DECAY(J)*TAUD)-174.D0)500,600,600
  500 IF(DABS(DECAY(J)*T)-174.D0)700,800,800
  700 IF(DABS(DECAY(J)*TAUC)-174.D0)900,1000,1000
  800 IF(DABS(DECAY(J)*TAUC)-174.D0)1100,1200,1200
  600 TERM(J)=0.D0
      GO TO 200
 1200 TERM(J)=DEXP(-DECAY(J)*TAUD)/(DECAY(J)*DECAY(J)*PI(J))
      GO TO 200
 1100 TERM(J)=(1.0D0-DEXP(-DECAY(J)*TAUC))*DEXP(-DECAY(J)*
     1TAUD)/(DECAY(J)*DECAY(J)*PI(J))
      GO TO 200
 1000 TERM(J)=(1.0D0-DEXP(-DECAY(J)*T))*DEXP(-DECAY(J)*TAUD)/
     1 (DECAY(J)*DECAY(J)*PI(J))
      GO TO 200
  900 TERM(J)=(1.0D0-DEXP(-DECAY(J)*T))*(1.0D0-DEXP(-DECAY(J)*
     1TAUC))*DEXP(-DECAY(J)*TAUD)/(DECAY(J)*DECAY(J)*PI(J))
  200 SUM(M)=SUM(M)+TERM(J)
      CALL SUMMTN (M,I)
  300 D(I)=D(I)+TERM2(M)
  400 SD=SD+D(I)
      RETURN
      END
```

```
      SUBROUTINE PRDCT (M,I)
      COMMON RAT(10),TEE(10),FRAC(10),DECAY(8),THALF(8),P(8),
     1PI(8),SUM(8),TERM(8),TERM2(8),MEMBR(8),T,TAUD,TAUC,N,L,
     1II
      DOUBLE PRECISION DECAY,THALF,P,PI,SUM,TERM,TERM2,T,TAUD,
     1TAUC,MEMBR,PCT(8),A(8),D(8),MEM1,RNEW(8),SNEW(8),SA,SD,
     1DEXP,DABS,PSUM,RAT,TEE,PROD,FRAC
      DO 100 J=M,I
      PI(J)=1.D0
      DO 101 K=M,I
      IF(K-J)102,101,102
102   PI(J)=PI(J)*(DECAY(K)-DECAY(J))
101   CONTINUE
100   CONTINUE
      RETURN
      END
```

```
      SUBROUTINE SUMMTN(M,I)
      COMMON RAT(10),TEE(10),FRAC(10),DECAY(8),THALF(8),P(8),
     1PI(8),SUM(8),TERM(8),TERM2(8),MEMBR(8),T,TAUD,TAUC,N,L,
     1II
      DOUBLE PRECISION DECAY,THALF,P,PI,SUM,TERM,TERM2,T,TAUD,
     1TAUC,MEMBR,PCT(8),A(8),D(8),MEM1,RNEW(8),SNEW(8),SA,SD,
     1DEXP,DABS,PSUM,RAT,TEE,PROD,FRAC
      TERM2(M)=0.D0
      PROD=1.D0
      M1=M
  299 PROD=PROD*DECAY(M1)
      IF(M1-I)301,302,302
  301 M1=M1+1
      GO TO 299
  302 PROD=PROD*P(M)
      TERM2(M)=PROD*SUM(M)
      RETURN
      END
```

```
      SUBROUTINE CALTAB
      COMMON RAT(10),TEE(10),FRAC(10),DECAY(8),THALF(8),P(8),
     1PI(8),SUM(8),TERM(8),TERM2(8),MEMBR(8),T,TAUD,TAUC,N,L,
     1II
      DOUBLE PRECISION DECAY,THALF,P,PI,SUM,TERM,TERM2,T,TAUD,
     1TAUC,MEMBR,PCT(8),A(8),D(8),MEM1,RNEW(8),SNEW(8),SA,SD,
     1DEXP,DABS,PSUM,RAT,TEE,PROD,FRAC
      PSUM=0.D0
    1 DO 2 I=1,N
      WRITE(3,3)MEMBR(I)
    3 FORMAT(@0@,//8X,A8,//)
      WRITE(3,4)
    4 FORMAT(@ COLLECT@,37X,@DELAY@,/,@ TIME(T)@,34X,
     1@TIME(TAUD)@,/)
      T=THALF(I)/1000.
      IF(L-I)201,200,200
  200 PSUM=PSUM+P(I)
  201 IB=0
    5 DO 6 M=1,20
      TAUD=THALF(I)/10.
      TAUC=THALF(I)
      DO 7 K=1,10
      TEE(K)=TAUD
      RAT(K)=0.D0
      CALL RATIO(A,SA)
      RAT(K)=A(I)/SA
      FRAC(K)=A(I)/PSUM
    7 TAUD=TAUD*1.77827941
      IB=IB+1
      GO TO (9,8),IB
    8 WRITE(3,10)  T,(RAT(K),K=1,10)
   10 FORMAT(1X,D9.3,2X,10(F6.4,4X))
      WRITE(3,13)(FRAC(K),K=1,10)
   13 FORMAT(12X,10(F6.4,4X))
      GO TO 6
    9 WRITE(3,12) (TEE(K),K=1,10)
   12 FORMAT(11X,10D10.3,/)
      GO TO 8
    6 T=T*1.77827941
    2 CONTINUE
      RETURN
       END
```

APPENDIX B

Analog Computer Solution and Flow Diagram

The solution of Equations 18 using a Pace, model TR-20, analog computer is presented in this section. The solution was used to test the results of the digital program ISOBAR for a ficticious decay chain and a comparison of the results is presented.

Consider the following ficticious decay chain consisting of five members and three production terms,

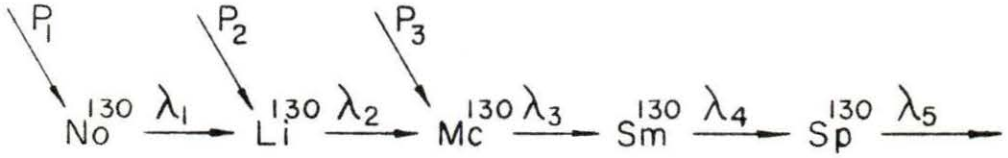

(1B)

where

$P_1 = 2 \times 10^9$ atom/sec $\qquad \lambda_1 = 0.693 \text{ sec}^{-1}$

$P_2 = 4 \times 10^9$ atom/sec $\qquad \lambda_2 = 0.1732 \text{ sec}^{-1}$

$P_3 = 2 \times 10^9$ atom/sec $\qquad \lambda_3 = 0.0433 \text{ sec}^{-1}$

$P_4 = 0 \qquad \lambda_4 = 0.0108 \text{ sec}^{-1}$

$P_5 = 0 \qquad \lambda_5 = 0.0027 \text{ sec}^{-1}$

Using the above values Equations 18 become

$$\frac{dA_1'}{dt} = 1.386 - 0.693\ A_1'$$

$$\frac{dA_2'}{dt} = 0.693 + 0.1732\ A_1' - 0.1732\ A_2'$$

$$\frac{dA_3'}{dt} = 0.0866 + 0.0433\ A_2' - 0.0433\ A_3' \qquad (2B)$$

$$\frac{dA_4'}{dt} = 0.0108\ A_3' - 0.0108\ A_4'$$

$$\frac{dA_5'}{dt} = 0.0027\ A_4' - 0.0027\ A_5'$$

where, due to magnitude scaling requirements,

$$A_i' = 10^{-9} A_i \; ; \; i = 1,5 \qquad (3B)$$

The TR-20 computer was programmed to solve Equations 2B. The flow diagram for the program is shown on Figure 14. The voltage inputs to the ganged switch at the upper left of the diagram simulate the radioactive isobars in the isotope separator beam. When the switch is closed the solution is analogous to the buildup of radioactive isobars on the tape of the moving tape collector. The length of time the switch is closed is the buildup time, T. When the switch is opened the solution is equivalent to terminating the collection of radioactive isobars at a particular point on the tape either by deflecting the isotope separator beam away from the deposit point, or by moving the tape away from the deposit point. The length of time the switch is opened is the decay time, τ_d.

The solution is obtained by placing the computer and a recorder in the operate mode with the beam switch closed. After the desired buildup time the switch is opened and the decay of the activity is recorded. Figure 15 shows a solution for Equations 2B and 3B for a buildup time of T = 20 seconds followed by a decay period. The point where the decay time equals 20 seconds is noted.

A solution of the decay chain activities using the digital program ISO-BAR was obtained for T = 20 seconds and TAUD = 20 seconds and the results were compared with the analog solution. The following table shows the results obtained:

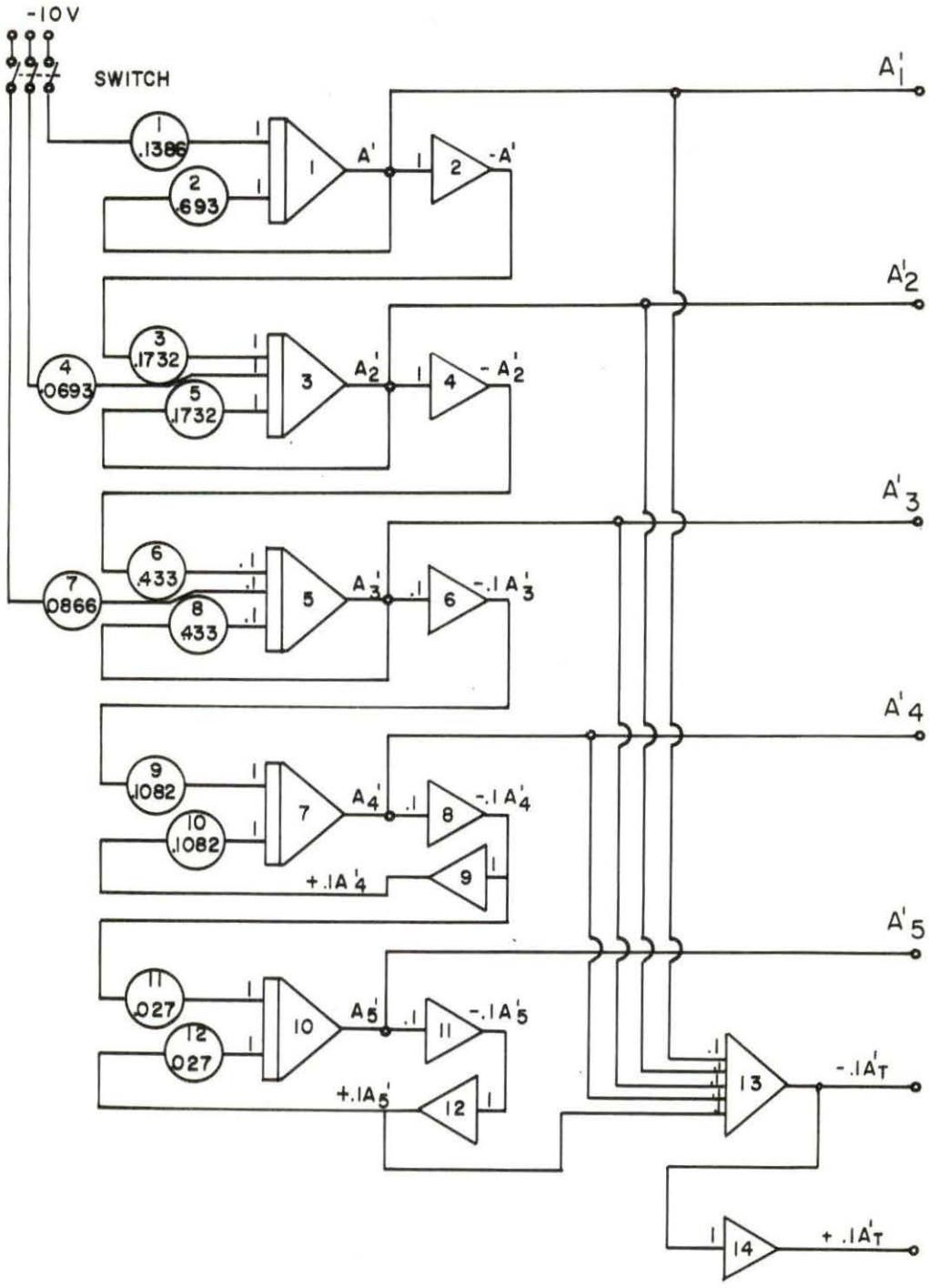

Figure 14. Analog program flow chart

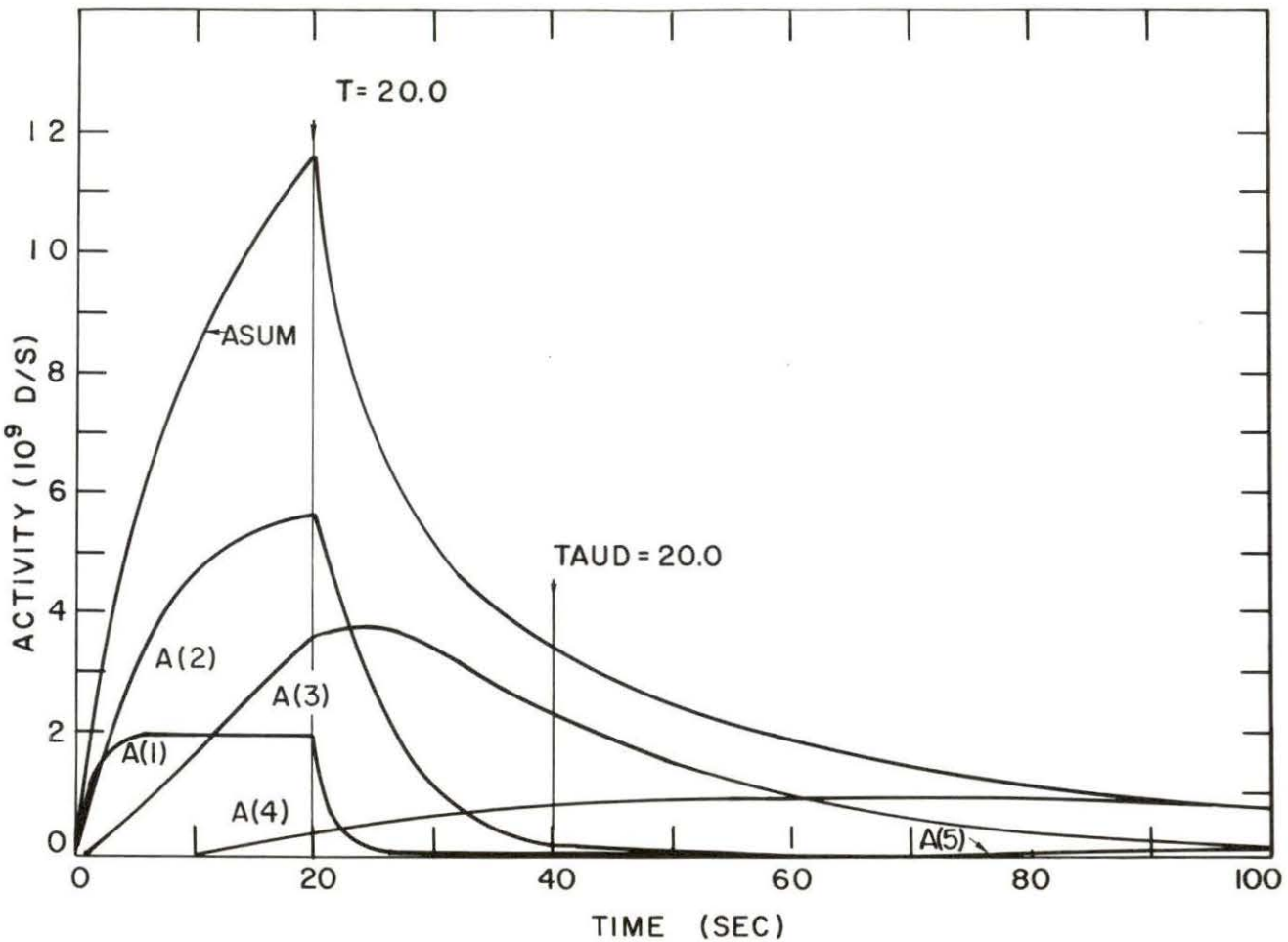

Figure 15. Analog solution of a three production term, fictional decay chain

Table 5. Comparison of analog solution and program ISOBAR results for $T = \tau_d = 20$ seconds

Fictional nuclide	Analog solution $A_i(T,\tau_d)$	ISOBAR solution $A_i(T,TAUD)$	Analog solution $R_i(T,\tau_d)$[a]	ISOBAR solution $R_i(T,TAUD)$
No^{130}	0	0.1913×10^4	0	0.5317×10^{-6}
Li^{130}	0.20×10^9	0.2022×10^9	0.0588	0.0562
Mc^{130}	2.35×10^9	2.413×10^9	0.6912	0.6707
Sm^{130}	0.90×10^9	0.9403×10^9	0.2660	0.2613
Sp^{130}	~ 0	0.4249×10^8	0	0.0118

[a]The value of $R_i(T,\tau_d)$ was obtained from Figure 15 by calculating the ratio of the individual activities to the total activity.

Since the accuracy of the analog computer is under the best conditions about $\pm$ 1%, when the amplifier output is less than about $\pm$ 0.5 volts (corresponding to $A_i(T,\tau_d) = 0.5 \times 10^9$ in this case) errors as large as $\pm$ 20% could be expected to occur. The agreement shown in Table 5 is thus reasonably close and indicates that the ISOBAR program functions properly.

APPENDIX C

The ISOMAX program listing appears on pages 67 through 76 in this section. The input parameters and format specifications are similar to the ISOBAR program. Also several of the subroutines called are the same as those called by the ISOBAR program and were described in Appendix A.

The operation of the program is easily determined by reference to the program listing and thus a flow chart is not included.

```
C
C
C    ---ISOMAX--- A PROGRAM FOR MAXIMIZING ACTIVITY SEPARATION
C                          IN DECAY CHAINS
C
C
      COMMON DECAY(8),P(8),PI(8),SUM(8),TERM(8),TERM2(8),T,
     1TAUD,N,L,II
      DOUBLE PRECISION MEMBR(8),MEM1,DECAY,P,PI,SUM,TERM,
     1 TERM2,T,TAUD,A(8),D1T(8),D2T(8),D1TAU(8),D2TAU(8),
     1FR(2),FRR(2,2),RNEW(8),ROLD(8),DELTA(2),FRFRR,FRSQ,SA,
     1SA2,SA4,SD1TAU,SD2T,SD1T,SD2TAU,DEXP,CONST,STEP,ROOT,
     1DSQRT,DABS,MULT,SAVT,SAVTAU
   13 READ(1,10001)MEM1,L,N
10001 FORMAT(A8,2I3)
      READ(1,1001)(MEMBR(J),J=1,N)
 1001 FORMAT(8A8)
10002 FORMAT(4D20.12)
      READ(1,10002) (DECAY(I),I=1,N),(P(I),I=1,L)
      WRITE(3,1002)MEM1
 1002 FORMAT(@1    CHAIN @,A8/)
10003 FORMAT(5X,@N=@,I5,10X,@DECAY CONSTANTS@,/)
      WRITE (3,10003) N
      WRITE (3,10002) (DECAY(I),I=1,N)
10004 FORMAT(5X,@L=@,I5,10X,@PRODUCTION CONSTANTS@,/)
      WRITE (3,10004) L
      WRITE (3,10002) (P(I),I=1,L)
      II=1
      T=0.25
      WRITE(3,1503)
 1503 FORMAT(10X,///)
      WRITE(3,1504)MEMBR(II)
 1504 FORMAT(10X,A8)
      WRITE(3,15005) II
15005 FORMAT(20X,@II=@,I3)
      WRITE(3,15008)
15008 FORMAT(5X,@TRIAL@,10X,@T@,23X,@TAUD@,21X,@RATIO@,18X,
     1@MOTOR SPD@,/)
      MM=0
  999 TAUD=0.0
      CALL RATIO(A,SA)
      ROLD(II)=A(II)/SA
      SPS=47.13/T
      WRITE(3,15009)MM,T,TAUD,ROLD(II),SPS
15009 FORMAT(5X,I3,2X,D20.12,5X,D20.12,5X,D20.12,5X,F10.4)
      TAUD=11.*T
      CALL RATIO(A,SA)
      ROLD(II+1)=A(II+1)/SA
      WRITE(3,15500)T,TAUD,ROLD(II+1)
15500 FORMAT(10X,D20.12,5X,D20.12,5X,D20.12,5X,@THIS IS 2ND@,
     1@ DET ACT SEP FOR 2ND MEMBER OF CHAIN@,/)
```

```
      T=T*1.414214
      MM=MM+1
      IF(T-47.)999,999,1
    1 II=II+1
11111 FORMAT (2D20.12)
      READ (1,11111) T,TAUD
      STEP=1.D0
      MM=0
      CALL RATIO (A,SA)
      ROLD(II)=A(II)/SA
      WRITE(3,1003)
 1003 FORMAT(10X,///)
      WRITE(3,1004)MEMBR(II)
 1004 FORMAT(10X,A8)
10005 FORMAT(20X,@II=@,I3)
      WRITE (3,10005) II
10006 FORMAT (10X,@STARTING RATIO=@,D20.12)
      WRITE (3,10006) ROLD(II)
10007 FORMAT (20X,@STARTING POINT AT T=@,D20.12,5X,@TAUD=@,
     1 D20.12)
      WRITE (3,10007) T,TAUD
  502 FORMAT (10X,@STARTING STEP SIZE=@,D20.12)
      WRITE(3,502) STEP
      WRITE(3,10008)
10008 FORMAT(5X,@TRIAL@,10X,@T@,23X,@TAUD@,20X,@RATIO@,18X,
     1@STEP SIZE@,/)
    2 CALL AT(SD1T,D1T)
      CALL ATAU(SD1TAU,D1TAU)
      CALL ATT(SD2T,D2T)
      CALL ATAUTA (SD2TAU,D2TAU)
      SA2=SA*SA
      SA4=SA**4
      FR(1)=(D1T(II)*SA-A(II)*SD1T)/SA2
      FR(2)=(D1TAU(II)*SA-A(II)*SD1TAU)/SA2
      FRR(1,1)=((D2T(II)*SA-A(II)*SD2T-D1T(II)*SD1T*2.0D0)*SA2
     1+A(II)*SA*SD1T*SD1T*2.0D0)/SA4
      FRR(1,2)=((D2T(II)*SA-D1T(II)*SD1TAU-D1TAU(II)*SD1T
     1-A(II)*SD2T)*SA2+A(II)*SA*SD1T*SD1TAU*2.0D0)/SA4
      FRR(2,1)=FRR(1,2)
      FRR(2,2)=((D2TAU(II)*SA-A(II)*SD2TAU-D1TAU(II)*SD1TAU*
     12.0D0)*SA2+A(II)*SA*SD1TAU*SD1TAU*2.0D0)/SA4
      FRFRR=FRR(1,1)*FRR(2,2)-FRR(1,2)*FRR(2,1)
      IF(FRFRR)6,12,6
    6 FRR(2,1)=FRR(1,1)
      FRR(1,1)=FRR(2,2)/FRFRR
      FRR(2,2)=FRR(2,1)/FRFRR
      FRR(1,2)=-FRR(1,2)/FRFRR
      FRR(2,1)=FRR(1,2)
      MM=MM+1
      CONST=0.D0
      DO 51 I=1,2
```

```
      DO 51 J=1,2
   51 CONST=CONST+FR(J)*FRR(J,I)*FR(I)
      IF(CONST)52,12,54
   52 CONST=-CONST
      ROOT=-1.0D0*DSQRT(CONST)
      GO TO 55
   54 ROOT=DSQRT(CONST)
   55 DO 56 I=1,2
      DELTA(I)=0.D0
      DO 56 J=1,2
   56 DELTA(I)=-(STEP/ROOT)*(FRR(I,J)*FR(J))+DELTA(I)
      SAVT=T
      SAVTAU=TAUD
   57 T=SAVT+DELTA(1)
      TAUD=SAVTAU+DELTA(2)
   66 CALL RATIO (A,SA)
      RNEW(II)=A(II)/SA
      IF(RNEW(II)-ROLD(II))63,19,62
   62 ROLD(II)=RNEW(II)
10009 FORMAT(5X,I3,2X,D20.12,5X,D20.12,5X,D20.12,5X,D20.12)
      WRITE (3,10009)MM,T,TAUD,RNEW(II),STEP
      GO TO 2
   63 IF(RNEW(II)-ROLD(II)+1.0D-9)58,19,19
   58 MULT=.5D0
      STEP=STEP*MULT
      DO 61 I=1,2
   61 DELTA(I)=MULT*DELTA(I)
      NN=1
      IF(DABS(DELTA(NN))-.1D-10)80,80,57
   80 IF(DABS(DELTA(NN+1))-.1D-10)19,19,57
10010 FORMAT(10X,@II=@,I3,5X,@MAXIMUM RATIO=@,D20.12)
   19 WRITE(3,10010) II,ROLD(II)
      IF(II+1-N)1,12,12
   12 GO TO 13
      END
```

```
      SUBROUTINE RATIO (A,SA)
      COMMON DECAY(8),P(8),PI(8),SUM(8),TERM(8),TERM2(8),T,
     1TAUD,N,L,II
      DOUBLE PRECISION A(8),DECAY,P,PI,SUM,TERM,TERM2,T,TAUD,
     1DEXP,SA,DABS
      SA =0.D0
      DO 400 I=1,N
      A(I)=0.D0
      LL=MIN0(I,L)
      DO 300 M=1,LL
      CALL PRDCT (M,I)
      SUM(M)=0.D0
      DO 200 J=M,I
      IF(DABS(DECAY(J)*T)-174.D0)500,600,600
500   IF(DABS(DECAY(J)*TAUD)-174.D0)700,900,900
600   IF(DABS(DECAY(J)*TAUD)-174.D0)800,900,900
900   TERM(J)=0.D0
      GO TO 200
800   TERM(J)=DEXP(-DECAY(J)*TAUD)/(DECAY(J)*PI(J))
      GO TO 200
700   TERM(J)=(1.0D0-DEXP(-DECAY(J)*T))*DEXP(-DECAY(J)*TAUD)/
     1  (DECAY(J)*PI(J))
200   SUM(M)=SUM(M)+TERM(J)
      CALL SUMMTN (M,I)
300   A(I)=A(I)+TERM2(M)
400   SA=SA+A(I)
      RETURN
      END
```

```
      SUBROUTINE AT(SD1T,D1T)
      COMMON DECAY(8),P(8),PI(8),SUM(8),TERM(8),TERM2(8),T,
     1TAUD,N,L,II
      DOUBLE PRECISION DECAY,P,PI,SUM,TERM,TERM2,T,TAUD,
     1SD1T,D1T(8),DEXP,DABS
      SD1T=0.D0
      DO 400 I=1,N
      D1T(I)=0.D0
      LL=MIN0(I,L)
      DO 300 M=1,LL
      SUM(M)=0.D0
      DO 200 J=M,I
      IF(DABS(DECAY(J)*(T+TAUD))-174.D0)500,600,600
600   TERM(J)=0.D0
      GO TO 200
500   TERM(J)=DEXP(-DECAY(J)*(T+TAUD))/PI(J)
200   SUM(M)=SUM(M)+TERM(J)
      CALL SUMMTN (M,I)
300   D1T(I)=D1T(I)+TERM2(M)
400   SD1T=SD1T+D1T(I)
      RETURN
      END
```

```
      SUBROUTINE ATAU(SD1TAU,D1TAU)
      COMMON DECAY(8),P(8),PI(8),SUM(8),TERM(8),TERM2(8),T,
     1TAUD,N,L,II
      DOUBLE PRECISION DECAY,P,PI,SUM,TERM,TERM2,T,TAUD,
     1SD1TAU,D1TAU(8),DEXP,DABS
      SD1TAU=0.D0
      DO 400 I=1,N
      D1TAU(I)=0.D0
      LL=MIN0(I,L)
      DO 300 M=1,LL
      SUM(M)=0.D0
      DO 200 J=M,I
      IF(DABS(DECAY(J)*T)-174.D0)500,600,600
500   IF(DABS(DECAY(J)*TAUD)-174.D0)700,900,900
600   IF(DABS(DECAY(J)*TAUD)-174.D0)800,900,900
900   TERM(J)=0.D0
      GO TO 200
800   TERM(J)=-DEXP(-DECAY(J)*TAUD)/PI(J)
      GO TO 200
700   TERM(J)=-(1.0D0-DEXP(-DECAY(J)*T))*DEXP(-DECAY(J)
     1*TAUD)/PI(J)
200   SUM(M)=SUM(M)+TERM(J)
      CALL SUMMTN (M,I)
300   D1TAU(I)=D1TAU(I)+TERM2(M)
400   SD1TAU=SD1TAU+D1TAU(I)
      RETURN
      END
```

```
      SUBROUTINE ATT(SD2T,D2T)
      COMMON DECAY(8),P(8),PI(8),SUM(8),TERM(8),TERM2(8),T,
     1TAUD,N,L,II
      DOUBLE PRECISION DECAY,P,PI,SUM,TERM,TERM2,T,TAUD,SD2T,
     1D2T(8),DEXP,DABS
      SD2T=0.D0
      DO 400 I=1,N
      D2T(I)=0.D0
      LL=MIND(I,L)
      DO 300 M=1,LL
      SUM(M)=0.D0
      DO 200 J=M,I
      IF(DABS(DECAY(J)*(T+TAUD))-174.D0)500,600,600
600   TERM(J)=0.D0
      GO TO 200
500   TERM(J)=-DECAY(J)*DEXP(-DECAY(J)*(T+TAUD))/PI(J)
200   SUM(M)=SUM(M)+TERM(J)
      CALL SUMMTN (M,I)
300   D2T(I)=D2T(I)+TERM2(M)
400   SD2T=SD2T+D2T(I)
      RETURN
      END
```

```
      SUBROUTINE ATAUTA(SD2TAU,D2TAU)
      COMMON DECAY(8),P(8),PI(8),SUM(8),TERM(8),TERM2(8),T,
     1TAUD,N,L,II
      DOUBLE PRECISION DECAY,P,PI,SUM,TERM,TERM2,T,TAUD,
     1SD2TAU,D2TAU(8),DEXP,DABS
      SD2TAU=0.D0
      DO 400 I=1,N
      D2TAU(I)=0.D0
      LL=MIN0(I,L)
      DO 300 M=1,LL
      SUM(M)=0.D0
      DO 200 J=M,I
      IF(DABS(DECAY(J)*T)-174.D0)500,600,600
500   IF(DABS(DECAY(J)*TAUD)-174.D0)700,900,900
600   IF(DABS(DECAY(J)*TAUD)-174.D0)800,900,900
900   TERM(J)=0.D0
      GO TO 200
800   TERM(J)=DECAY(J)*DEXP(-DECAY(J)*TAUD)/PI(J)
      GO TO 200
700   TERM(J)=DECAY(J)*(1.0D0-DEXP(-DECAY(J)*T))*
     1DEXP(-DECAY(J)*TAUD)/PI(J)
200   SUM(M)=SUM(M)+TERM(J)
      CALL SUMMTN (M,I)
300   D2TAU(I)=D2TAU(I)+TERM2(M)
400   SD2TAU=SD2TAU+D2TAU(I)
      RETURN
      END
```

```
      SUBROUTINE SUMMTN(M,I)
      COMMON DECAY(8),P(8),PI(8),SUM(8),TERM(8),TERM2(8),T,
     1TAUD,N,L,II
      DOUBLE PRECISION DECAY,P,PI,SUM,TERM,TERM2,T,TAUD,
     1PROD,DEXP
      TERM2(M)=0.DO
      PROD=1.DO
      M1=M
  299 PROD=PROD*DECAY(M1)
      IF(M1-I)301,302,302
  301 M1=M1+1
      GO TO 299
  302 PROD=PROD*P(M)
      TERM2(M)=PROD*SUM(M)
      RETURN
      END
```

```
      SUBROUTINE PRDCT (M,I)
      COMMON DECAY(8),P(8),PI(8),SUM(8),TERM(8),TERM2(8),T,
     1TAUD,N,L,II
      DOUBLE PRECISION DECAY,P,PI,SUM,TERM,TERM2,T,TAUD,DEXP
      DO 100 J=M,I
      PI(J)=1.DO
      DO 101 K=M,I
      IF(K-J)102,101,102
  102 PI(J)=PI(J)*(DECAY(K)-DECAY(J))
  101 CONTINUE
  100 CONTINUE
      RETURN
      END
```